



**MARMARA UNIVERSITY
INSTITUTE FOR GRADUATE STUDIES
IN PURE AND APPLIED SCIENCES**



**COPPER REMOVAL FROM AMMONIACAL
SPENT ETCHANT BY USING MAGNETIC**

NANOPARTICLES

OUMER ALI YASSIN

MASTER THESIS

Department of Environmental Engineering

Thesis Supervisor
Prof. Dr. Zehra Semra Can

ISTANBUL, 2016



**MARMARA UNIVERSITY
INSTITUTE FOR GRADUATE STUDIES
IN PURE AND APPLIED SCIENCES**



**COPPER REMOVAL FROM AMMONIACAL
SPENT ETCHANT BY USING MAGNETIC**

NANOPARTICLES

**OUMER ALI YASSIN
(524312921)**

MASTER THESIS
Department of Environmental Engineering

Thesis Supervisor
Prof. Dr. Zehra Semra Can

ISTANBUL, 2016

**MARMARA UNIVERSITY
INSTITUTE FOR GRADUATE STUDIES IN
PURE AND APPLIED SCIENCES**

OUMER ALI YASSIN, a Master of Science student of Marmara University Institute for Graduate Studies in Pure and Applied Sciences, defended his thesis entitled “**COPPER REMOVAL FROM AMMONIACAL SPENT ETCHANT BY USING MAGNETIC NANOPARTICLES**”, on October 05, 2016 and has been found to be satisfactory by the jury members.

Jury Members

Signature

Prof. Dr. Zehra Semra Can

(Advisor)



Prof. Dr. Nihal Bektaş

(Jury Member)



Yrd. Doç. Dr. Esra Edrim

(Jury Member)




APPROVAL

Marmara University Institute for Graduate Studies in Pure and Applied Sciences Executive Committee approves that **OUMER ALI YASSIN** be granted the degree of Master of Science in Department of Environmental Engineering, Environmental Engineering Program on *24.10.2016*

(Resolution no: *2016/24-9.2*)

Director of the Institute

Prof. Dr. Uğur YAHSİ



ACKNOWLEDGEMENT

I would like to express my deepest appreciation to my advisor, Prof. Dr. Zehra Semra CAN, for her guidance and advices from the early stages of my Master's degree. And also, I would like to thank her for suggesting this excellent research topic as the subject of my thesis. She extended continuous encouragement and unforgettable support throughout the study and contributed a lot to the success of my thesis. This thesis would never be completed without her proper direction and continuous help.

I would also like to thank research assistance, Gül Gülenay HACIOSMANOĞLU, for her great contribution and limitless help with showing me every step of the lab work without boring. My deepest thank also goes to Assist. Prof. Dr. Seval GENÇ, for her support in the production of magnetic nanoparticles. I wish to say thank you to my intimate friend Ebrahim Tilahun for his help with writing the thesis.

I would like to thank my family members for their endless love, support and praying till the end of my research. I am extremely grateful to my beloved wife Nuralah Seid. You supported me with your love and energy in any possible way and you gave me the strength and motivation to continue during the time of difficulty. This thesis is the result of your patience.

Lastly, I would like to thank Marmara University Scientific Research Fund (BAPKO) for its financial support for this study within the Project no: FEN-A-100713-0321.

September, 2016

Oumer Ali Yassin

TABLE OF CONTENTS

	PAGE
ACKNOWLEDGEMENT	i
ABSTRACT	iv
ÖZET	v
SYMBOLS	vi
ABBREVIATIONS	ix
LIST OF FIGURES	xi
LIST OF TABLES	xiii
1. INTRODUCTION	1
1.1. Scope of the Study.....	1
1.2. Objectives of the Study	3
1.3. General Background.....	3
1.3.1. Printed circuit boards (PCBs)	3
1.3.1.1. PCBs production in the world	3
1.3.1.2. Chemical compositions of PCBs.....	5
1.3.1.3. PCB manufacturing processes	5
1.3.1.4. Quantity of waste PCBs generation	7
1.3.1.5. Waste PCBs and the environment.....	9
1.4. Chemical Etching	10
1.4.1. Copper etchants in PCB manufacturing	11
1.4.1.1. Ferric chloride (FeCl ₃) etchant.....	11
1.4.1.2. Cupric chloride (CuCl ₂) etchant	12
1.4.1.3. Alkaline (Ammoniacal) etchant	13
1.5. Spent Etchant.....	14
1.6. Copper in Wastewaters.....	16
1.6.1. Copper removal methods from wastewaters	16
1.7. Magnetic Nanoparticles (MNPs).....	17
1.7.1. Applications of iron oxide nanoparticles	17

1.7.1.1. Medical application of IONPs.....	18
1.7.1.2. Environmental applications of IONPs	18
1.7.2. Surface coating (modification) of nanoparticles	19
1.7.3. Removal of Cu ²⁺ ions from wastewaters using surface coated MNPs	19
1.7.4. Important properties of magnetic nanoparticles	20
1.7.4.1. Crystallite size.....	20
1.7.4.2. Zeta potential.....	20
1.7.4.3. Point of zero charge	22
1.7.5. Characterization of magnetic nanoparticles	22
1.7.5.1. Scanning and transmission electron microscopy (SEM and TEM)	22
1.7.5.2. X-ray diffraction (XRD)	23
1.7.5.3. Fourier transform infra-red spectroscopy (FTIR)	23
2. MATERIALS AND METHODS	24
2.1. Materials.....	24
2.2. Methods.....	24
2.2.1. Preparation of synthetic spent etchant (Copper stock solution)	24
2.2.2. Production of magnetite iron oxide (Fe ₃ O ₄) MNP	24
2.2.3. Batch adsorption study	27
3. RESULTS AND DISCUSSIONS.....	28
3.1. Adsorption Studies Results	28
3.1.1. Effect of MNP amount on adsorption.....	31
3.2. Results of Point of Zero Charge.....	32
3.3. Results of FTIR Analysis	34
3.4. Discussions.....	42
4. CONCLUSIONS	45
REFERENCES.....	47

ABSTRACT

COPPER REMOVAL FROM AMMONIACAL SPENT ETCHANT BY USING MAGNETIC NANOPARTICLES

The aim of this study was to evaluate Cu^{2+} ions adsorption capacities of bare and polymer coated Fe_3O_4 magnetic nanoparticles (MNPs) from ammoniacal spent etchant wastewater. For this purpose, Fe_3O_4 MNPs were produced and coated with chitosan, polyvinyl-pyrrolidone (PVP), oleic acid and polyvinyl alcohol (PVA) polymers. The maximum copper adsorptions capacities obtained by these coated MNPs at 20°C and pH 9.5 were 204.6 mg/g, 189.3 mg/g, 165.3 mg/g and 160.7 mg/g respectively. Whereas the Cu^{2+} adsorption capacities of the laboratorial and commercial (Aldrich) bare Fe_3O_4 MNPs were only 23.6 mg/g and 15.4 mg/g respectively. The FTIR analysis demonstrated that the polymers were successfully coated on the surface of Fe_3O_4 MNP. Zeta potential results showed the pH of point of zero charge of the uncoated MNPs was around 3.8. However, all the MNPs used in this study showed negative zeta potentials at pH around 9.5 indicating more Cu^{2+} ions could be adsorbed on the surface of the MNPs. Generally, the results of this study was consistent with reported data and it can be concluded that surface coated Fe_3O_4 MNPs can provide better adsorption results than the uncoated MNPs and can widely be used in the adsorption studies for the removal of copper and other heavy metals from water and wastewaters.

September, 2016

Oumer Ali Yassin

ÖZET

MANYETIC NANOPARTIKULLER KULLANARAK AMONYAKLI ASINDIRICI ATIK SIVILARDAN BAKIR IYONU (CU²⁺) GIDERİM

Bu çalışmanın ana amacı kapsız ve polimer kaplı Fe₃O₄ manyetik nanoparçacıkların (MNP) amonyaklı aşındırıcı atık sıvılardan bakır iyonu (Cu²⁺) giderim kapasitesini değerlendirmektir. Bu amaca yönelik olarak, Fe₃O₄ manyetik nanoparçacıkları üretilerek kitosan, polivinil pirolidon (PVP), oleik asit ve polivinil alkol (PVA) polimerleri ile kaplanmıştır. 20 °C sıcaklık ve pH 9.5 koşullarında elde edilen maksimum bakır adsorpsiyon kapasiteleri sırasıyla 204.6 mg/g, 189.3 mg/g, 165.3 mg/g ve 160.7 mg/g olarak ölçülmüştür. Buna karşılık, hem laboratuvarımızda hazırlanmış olan hem de ticari olarak satılan (Aldrich) kapsız Fe₃O₄ manyetik nanoparçacıklarının adsorpsiyon kapasiteleri sadece 23.6 mg/g ve 15.4 mg/g olduğu laboratuvar çalışmaları ile ortaya konmuştur. FTIR analizi, polimerlerin Fe₃O₄ MNP yüzeyine başarılı olarak kaplandığını göstermiştir. Zeta potansiyel sonuçları, kapsız MNP'lerin sıfır yük noktası pH'ının (pHpzc) 3.8 civarında olduğunu göstermiştir. Bununla birlikte bu çalışmada kullanılan tüm MNP'ler pH 9.5 civarında negatif zeta potansiyel değeri göstermiş olup bu durum daha fazla Cu²⁺ iyonunun MNP yüzeyine adsorplanabilirliği anlamına gelmektedir. Genel olarak, bu çalışmada elde edilen sonuçlar, literatürdeki sonuçlarla uyumludur ve yüzeyi polimer ile kaplanmış Fe₃O₄ MNP'lerin kapsız MNP'lere göre daha iyi adsorpsiyon sağlayabildiği ve bu MNP'lerin su ve atıksularda bakır ve diğer ağır metallerin giderimine yönelik adsorpsiyon çalışmalarında kullanılabileceği sonucuna varılmıştır.

September, 2016

Oumer Ali Yassin

SYMBOLS

Ag	:Silver
Au	:Gold
BeO	:Beryllium Oxide
C_e	:Final Concentration
CH ₃ Br	:Methyl Bromide
cm ⁻¹	:Per/Centimeter
Cu ²⁺	:Copper(II) ion
CuCl ₂	:Cupric Chloride
CuCl ₂ .2H ₂ O	:Dehydrate Copper Chloride
CuO	:Copper Oxide
Cu(OH) ₂	:Copper Hydroxide
Fe ^{II}	:Iron (II)
Fe ^{III}	:Iron (III)
FeCl ₃	:Ferric Chloride
Fe ₃ O ₄	:Magnetite Iron Oxide
γ-Fe ₂ O ₃	:Maghemite Iron Oxide
HCl	:Hydrochloric Acid
HClO ₄	:Chlorate
H ₂ O	:Water
K	:Kelvin

Mg	:Milligram
mg/g	:Millgram per Gram
mg/kg	:Milligram per Kilogram
mg/L	:Milligrams per liter
Mid	:Middle
Min	:Minutes
Mm	:Micro meter
Mol	:Molarity
mole/g	:Mole per gram
mole/L	:Mole per Liter
NaOH	:Sodium Hydroxide
NaHClO ₄	:Sodium Chlorate
NH ₂	:Ammine
NH ₃	:Ammonia
NH ₄ Cl	:Ammonium Chloride
NH ₄ OH	:Ammonium Hydroxide
(NH ₄) ₂ SO ₄	:Ammonium Sulfate
nm	:Nano Meter
Pb	:Lead
Pd	:Palladium
Pt	:Platinum

pH	:Power (Potential) of Hydrogen
q_e	:Adsorption
q_{max}	:Maximum Adsorption
Sn	:Tin
°Bé	:Baumé
°C	:Degree Celsius
°F	:Degree Fahrenheit
μm	:Micro Meter
\$:dollar
ζ	:Zeta Potential
[]	:square bracket
{ }	:braces

ABBREVIATIONS

AAS	:Atomic Absorption Spectroscopy
BAN	:Basel Action Network
B.C.	:Before Christ
PBDEs	:Poly Brominated Diphenyl Ethers
PBDD/Fs	:Polybrominated dibenzo-p-dioxins/ furans
BFRs	:Brominated Flame-Retardants
CM- β -CD	:CarboxyMethyl- β -CycloDextrin
(Fe ⁰ /nZVI)	:Nanoscale Zero Valent Iron
FTIR	:Fourier Transform Infra-Red Spectroscopy
INP	:Iron-based Nanoparticle
IONP	:Iron Oxide Nanoparticles
IOMNPs	:Iron Oxide Magnetic Nanoparticles
Lab	:Laboratory
MFs	:Metallic Fractions
MNP	:Magnetic Nanoparticle
MRI	:Magnetic Resonance Imaging
NMFs	:Nonmetallic Fractions
NP	:Nano Particle
PAHs	:Polycyclic Aromatic Hydrocarbons
PCB	:Printed Circuit Board

pH _{pzc}	:pH of Point of Zero Charge
PTH	:Plated Through Holes
PVA	:polyvinyl Alcohol
PVC	:Poly Vinyl Chloride
PVP	:PolyVinyl Pyrrolidone
PWB	:Printed Wiring Board
P _{zc}	:Point of Zero Charge
rpm	:Revolution per minute
SEM	:Scanning Electron Microscopy
TEM	:Transmission Electron Microscope
TRI	:Toxic Release Inventory
US	:United States
UNEP	:United Nations Environment Programme
WEEE	:Waste Electric and Electronic Equipment
WHO	:World Health Organization
XPS	:X-ray Photoelectron Spectroscopy
XRD	:X-Ray Diffraction

LIST OF FIGURES

	PAGE
Figure 1.1. The world PCB manufacturing progression	4
Figure 1.2. Major PCB producing countries in 2011	5
Figure 1.3. Double- sided PCB design on a computer	5
Figure 1.4. The two processing methods used to produce a double-sided PCB.....	6
Figure 1.5. WEEE importing and exporting traffic routes of Asian countries.....	7
Figure 1.6. Proportions of wastes generated from PCB manufacturing in Taiwan	9
Figure 1.7. Air and water emission release weight percent for select chemicals from the US PCB industry in 2006	10
Figure 1.8. A general etching process to remove unwanted copper from PCBs board.....	11
Figure 1.9. Simplified scheme of the utilization of iron oxide nanoparticles (IONP) for the remediation of polluted groundwater.....	18
Figure 1.10. Schematic model of surface modification of iron oxide.....	19
Figure 1.11. Chemical structures of Fe ₃ O ₄ and the polymers used in this study.....	20
Figure 1.12. Illustration for ions Distributed around a charged particle.....	21
Figure 1.13. Interparticle potential versus interparticle distance	21
Figure 2.1. The produced synthetic spent etchant solution	24
Figure 2.2. MNP production process	26
Figure 3.1. Blank and MNP added samples	29
Figure 3.2. C _e versus q _e graph	29
Figure 3.3. Metals adsorption mechanism by chitosan coated MNP.....	31
Figure 3.4. Effect of MNPs dose on the adsorption of Cu ²⁺ ions.....	31
Figure 3.5. Zeta potential of samples at various pH ranges.....	33

Figure 3.6. FTIR studies of bare Fe ₃ O ₄ , pure chitosan and chitosan coated Fe ₃ O ₄	34
Figure 3.7. Bond formation between amino group (NH ₂) of chitosan and Fe ₃ O ₄	36
Figure 3.8. FTIR studies of bare Fe ₃ O ₄ , pure oleic acid & oleic acid coated Fe ₃ O ₄	36
Figure 3.9. Bond formation between oleic acid and iron atom.....	38
Figure 3.10. FTIR studies of bare Fe ₃ O ₄ , pure PVA and PVA coated Fe ₃ O ₄	38
Figure 3.11. FTIR studies of bare Fe ₃ O ₄ , pure PVP and PVP coated Fe ₃ O ₄	40
Figure 3.12. FTIR studies of the two uncoated Fe ₃ O ₄ MNPs	41

LIST OF TABLES

	PAGE
Table 1.1. Amount of waste from multi-layer PCB manufacturing process in Taiwan.....	8
Table 1.2. Contents of spent ammoniacal (alkaline) etchant wastewater.....	15
Table 3.1. Results of batch adsorption experiments.....	30
Table 3.2. Comparison of the results with literature data.....	32
Table 3.3. FTIR spectra of pure iron oxide, chitosan, and chitosan coated iron oxide.....	35
Table 3.4. FTIR spectra of pure iron oxide, oleic acid, and oleic acid coated iron oxide.....	37
Table 3.5. FTIR spectra of pure iron oxide, pure PVA, and PVA coated iron oxide.....	39
Table 3.6. FTIR spectra of pure iron oxide, PVP, and PVP coated iron oxide.....	40
Table 3.7. FTIR spectra of lab. Produced and Aldrich iron oxide.....	42

1. INTRODUCTION

1.1. Scope of the Study

Contamination of water with heavy metals released from different industries like mining, metal finishing and plating plants is becoming severe problem for both environment and humans [1]. The main problem of heavy metals is that they are persistent for a longer period of time without degradation and cause harmful effects through food chain [2]. Cr, Hg, Cu, Ni, Zn and Cd are among the major heavy metals that can bring severe problems [3].

Copper, which is the major effluents in industrial wastewaters, is among the essential elements required for normal structure and function of cells. However, if it is in excess, it causes abnormalities for the proper activities of cells [4]. For example, if the level of copper in drinking water is more than 2 mg/L, it could cause stomach, liver and kidney damages [5]. In addition, excessive ingestion of copper in human diet results in vomit, cramps, and even death [6]. The World Health Organization (WHO) limits its amount in drinking water to be 2 mg/L [7].

Spent etchant is the industrial wastewater produced from the etching step of Printed Circuit Board (PCB) industries and it contains high amount of copper [8]. PCBs are the main parts of electronic materials, and the world electronic products reached 40 billion US dollars in 2009 [9]. The annual PCB production in the world is estimated to be approaching to 300 million m² [10], from this 0.7 million m³ of the waste is produced every year [11]. The total metallic content of PCBs is 28%, of which copper, lead and nickel consist 10-20%, 1-5% and 1-3%, respectively [12].

Etching is one of the major technical steps involved in the production of PCBs. In the design of PCB, the uncovered copper is dissolved in a chemical called etchant so that the required PCB design is produced. Ferric chloride, hydrogen peroxide, cupric chloride and ammoniacal (alkali) etchants are some of the chemicals which have been used in etching processes. Among these, the alkaline etchant is the most common etchant used in most PCB industries due to its best etching efficiency [13].

Spent ammoniacal etchant solution is an alkaline hazardous waste solution produced during the etching of copper with ammoniacal etchant. The solution has pH of 8.5-9.5, copper concentration of 130-160g/L, chloride concentration of 175-190g/L, ammonia concentration of 170-201g/L and a molar ratio of ammonia to copper 4:1. The waste also consists of additional chemicals required for the etching process [14].

The presence of ammonia and other heavy metals in the solution make it hazardous and cause health and environmental problems. The most difficult problem of the solution is caused by due to the complex formed between copper and ammonia. Copper ammonia complex $[\text{Cu}(\text{NH}_3)_4^{2+}]$ is the major complex specie formed in spent ammoniacal etchant. The complex is very difficult to break and prevents the precipitation of metal [15]. If this waste solution is disposed before treating, it can bring a complicated environmental and human problems. In addition, from the economical point of view, the copper and the spent etchant can be recovered and recycled for further use. Thus, the rapid and effective copper removal is among the major concern in wastewater treatment.

Numerous technologies like chemical precipitation, ion exchange and membrane filtration are used for the removal of Cu^{2+} from wastewaters [16]. However, these conventional methods commonly have several drawbacks in relation with cost, time and complexity [17]. For this reason, it is needed to find other methods that are simple and cheap.

In recent years, adsorption of Cu^{2+} ions using magnetic nanoparticles (MNPs) is becoming more attractive method for copper removal from different wastewaters due to its simplicity and cost effectivity [18]. In addition, their small size and high surface-area-to volume ratio make them preferable for the removal of heavy metals from polluted water streams [19]. Moreover, if the MNPs are coated, their adsorption capacities increase because of the existence of various functional groups which can bind the targeted metals. [20].

In this study, the bare and various polymer coated Magnetite Iron Oxide (Fe_3O_4) MNPs were used to analyze their adsorption efficiencies of Cu^{2+} ions from ammoniacal spent etchant. The polymers used to coat the MNP were chitosan, polyvinyl-pyrrolidone (PVP), oleic acid and polyvinyl alcohol (PVA). The commercial Fe_3O_4 MNP (Aldrich) was also used to assess its adsorption efficiency in respect to the MNP produced in our university. The characterizations of

the MNPs were studied using FTIR (Fourier Transform Infra-Red Spectroscopy). The synthetic ammoniacal spent etchant (copper stock solution) was prepared by Environmental Engineering department, where as the MNPs were produced by Metallurgical and Materials Engineering department of Marmara University as described in Chapter 2.

1.2. Objectives of the Study

The feasibility of MNP for selective removal of copper was studied by a number of researchers. However, these studies targeted on the treatment of wastewater with low copper content. To date, treatment of wastewater from PCB industries with very high copper concentration around 170 g/L, in which copper forms complex in the form of $\text{Cu}(\text{NH}_3)_4^{2+}$ is carried out. Therefore, the main objective of the study was to determine the bare and polymer coated Magnetite Iron Oxide (Fe_3O_4) MNPs for their adsorption efficiencies of Cu^{2+} ions from ammoniacal (alkaline) spent etchant wastewater with low operation cost and without generating secondary waste for PCB manufacturers. Furthermore, the adsorption capacities of the Fe_3O_4 MNP produced in our university and the commercial Fe_3O_4 (Aldrich) MNP were also compared.

1.3. General Background

1.3.1. Printed circuit boards (PCBs)

Printed Circuit Boards (PCBs) are the main components of any electronic, communications, defense and automotive manufacturer designed for the linkage of electrical signals among different parts [21]. PCBs are also called as Printed Wiring Boards (PWBs) due to their ability to supply electrical wiring on a rigid surface [22]. Therefore, PCBs are electrical circuit systems formed by putting electrical parts on a non-conductive board to create conduction among different parts with metal coating [23]. The manufacture of PCBs uses different precious metals such as Au, Ag, Pd and Pt in its different steps which make waste PCBs is an important waste from the view of economy [24].

1.3.1.1. PCBs production in the world

The increment of the production of electronic materials is the indirect indication of the fast growth of the PCB business [25]. About \$1 trillion is obtained from the sale of electronic

products each year. Nevertheless, the US PCB business had decreased from 42% in 1984 to 10% in 2006. In 2000, the number of employees in US PCB industries was about 80,000, but it showed 50% reduction in 2004. The reduction can lead to the conclusion that the production shifted from the US to other countries.

Currently, Asia produces 75% of the global PCBs, with more than 1000 PCB industries found in China. In 2003, Japan was the first, China the second, US the third, Taiwan the fourth, Europe the fifth, and South Korea the sixth world largest PCB producers at 29%, 17%, 15%, 13%, 10%, and 8%, respectively. China took the leader of the world PCB producer in 2006, and it accounts 25% of the world total PCBs [22]. The global trend in the investment of PCB industries and prediction growth is shown in Figure 1.1.

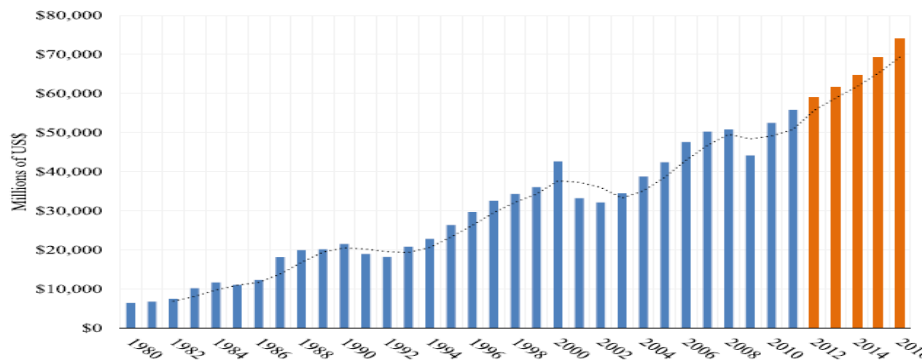


Figure 1.1. The world PCB manufacturing progression [26]

As it is seen from the figure, the world PCB production is increasing dramatically which covered less than 10,000 million US dollar in the years 1980 and estimated to be increased to 80,000 million US dollar in the years 2016. From this figure, it can be concluded that the PCB manufacturing business will increase in the future, and ultimately the waste PCBs generation will also increase [26].

The major PCB producers are shown by Figure 1.2. From the graph it is seen that China is the largest PCB producer, which produced 23, 561 million US dollar, whereas Hong Kong produced 138 million US dollar PCB in the year 2011, which made them the leading country and the least region in the production of PCB in this year [27]. According to the study conducted, the rate of global PCBs production rate is 8.7% [28].

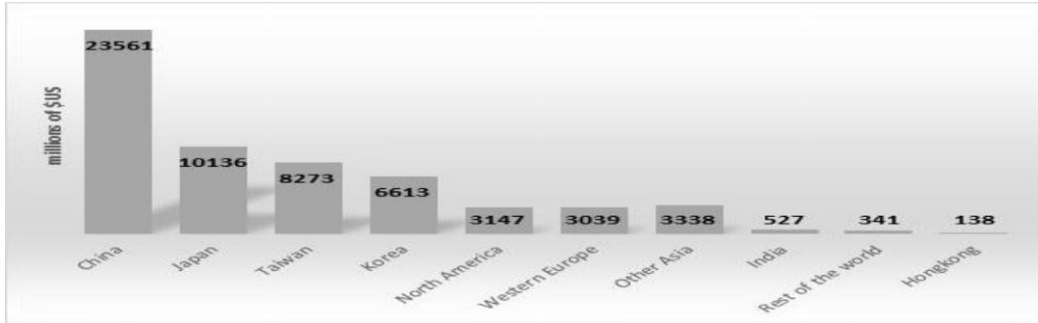


Figure 1.2. Major PCB producing countries in 2011 [27].

1.3.1.2. Chemical compositions of PCBs

The contents of PCBs are determined by the kind of PCBs and their functions. Generally, around 28% of PCBs is composed of metals, 23% plastics and 48% is ceramics and glass materials [29]. In addition, resin and various kinds of hardeners are used to form thermoset plastics [30]. Copper is the major element used for the formation of conducting layer among other metals due to its high conductivity properties. Precious metals such as Pt are also present in switches and sensors [31]. According to the report, more than half of the total copper production is used in the application of electronic manufactures [32]. Most of the plastic substances found in PCB contain polymers and halogenated compounds which are believed to be carcinogenic [24]. Antimony trioxide is found with polymers as flame retardant [33].

1.3.1.3. PCB manufacturing processes

PCB production is most complicated and the process needs more than 50 technical steps [34]. Based on the design, PCBs can be grouped as single, double or multi-layered. In the first two groups of PCBs, the conducting layer is on one or both sides and mostly found in automotive electronics [35]. Multilayer boards account more than 65% of the US PCB production [36]. Each produced PCB board has a particular circuit design arranged for the desired electronic product system [21]. Figure 1.3 shows double-sided PCB design on a computer.

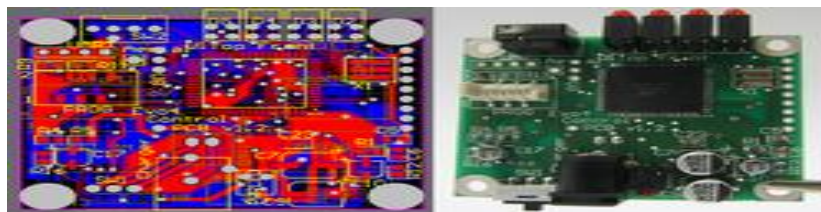


Figure 1.3. Double- sided PCB design (left) and board assembly (right) on a computer [37].

Major PCB manufacturing steps regardless of design, involve board drilling and preparation, image transfer of the dry film, copper etching and electroplating [21]. As it is shown in Figure 1.4, pattern plate and panel plate are two methods for the production of double-sided PCB [37].

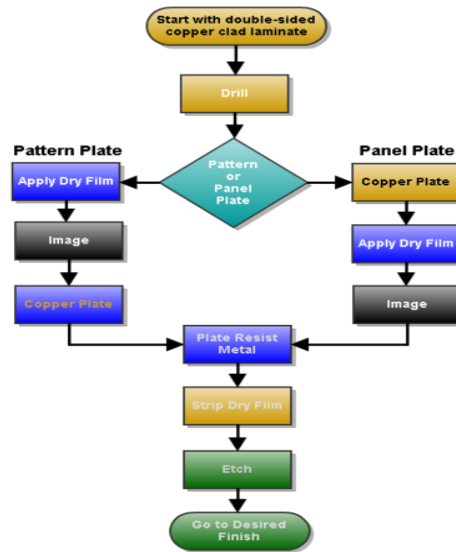


Figure 1.4. The two known processing methods used to produce a double-sided PCB.

The common processes of PCB manufacturing are briefly explained in the following paragraphs: Holes are drilled into PCBs to give support for the connection of layers on the circuits. Copper is plated onto the holes to make them conductive.

The circuit layer image is transferred from the film to copper foil of the PCB material by the process called image transfer. Image transfer for inner layers involves imaging, developing, and etching, and the application of photoresist that is used as the etch resist. Whereas, for the outer layer, it involves the electroplating of copper by precious metals like lead, tin and gold. [38].

The other common process of PCBs production is metal plating. In this step copper is coated with tin–lead layer. The unnecessary copper layer is removed by etching chemicals. In PCB industries, more than 90% of the discharged copper originates from the etching process. Then, tin–lead layer found on the upper part is stripped and the panel is covered with solder resist [39]. Finally, the panel is rinsed and washed in 10% H₂SO₄ for the prevention of oxidation before ready for the market [40].

1.3.1.4. Quantity of waste PCBs generation

The world increasing rate of PCBs manufacturing results in the increasing of waste PCBs. The UN Environment Programme (UNEP) report says 20–50 million tons of waste electric and electronic equipment (WEEE) are produced every year and this is higher than other municipal wastes [41]. It was also reported that the electronics waste accounted 4% and 8% of municipal solid waste in the year 2002 [42] and 2005[43], respectively.

China is under great problem with WEEE disposal both from internal production and external transfer as shown in Figure 1.5. Large quantities of WEEE are imported to China from different countries. According to the report, more than 50 % of the total collected domestic WEEE [44] and 10 million useless computers in USA in 2002 were moved to Asian countries such as China for recycling. The study also showed that from the total WEEE exported to Asia, more than 90% is discarded in China. Therefore, the largest amount of WEEE is found in china, which accounts about 70% the world annual WEEE [45]. In China alone, more than half million tons of waste PCBs is treated annually [46].



Figure 1.5. WEEE importing and exporting traffic routes of Asian countries [45].

In general, the wastes generated from PCB industry can be grouped as solid and liquid wastes. Solid wastes include copper clad, protection film, drill dust, waste board, etc., whereas the liquid wastes include spent solutions, washing solutions and resistor [47]. In PCBs production, the common hazardous waste streams are spent solutions, spent rinse water and other metal-laden

wastewaters [40] originated from waste rinsing water, waste etchant and discharge of waste electroplating solutions [48]. Table 1.1 shows the amount of waste generated from a typical multi-layer PCB process in Taiwan. From the table it is clearly seen that more than 65% of the wastes generated from this PCB industry is hazardous which can cause health and environmental problems.

Table 1.1. Amount of waste generated from PCB manufacturing process in Taiwan [47].

Wastes	Wastes Characterization	kg/m ² of PCB
Waste board	Hazardous	0.01~0.3kg/m ²
Edge trim	”	0.1~1.0kg/m ²
Hole drilling dust	”	0.005~0.2kg/m ²
Copper powder	Non-hazardous	0.001~0.01kg/m ²
Tin/lead dross	Hazardous	0.01~0.05kg/m ²
Copper foil	Non-hazardous	0.01~0.05kg/m ²
Film	”	0.1~0.4kg/m ²
Drill backing board	”	0.02~0.05kg/m ²
Wastewater treatment slurry	Hazardous	0.02~3.0kg/m ²
Acidic etching solution	”	1.5~3.5 L/m ²
Basic etching solution	”	1.8~3.2 L/m ²
Rack stripping solution	”	0.2~0.5 L/m ²
Tin/lead stripping solution	”	0.2~0.6 L/m ²
Sweller solution	”	0.05~0.1 L/m ²
Flux solution	”	0.05~0.1 L/m ²
Microetching solution	”	1.0~2.5 L/m ²
PTH copper solution	”	0.2~0.5 L/m ²

Moreover, the percentage of major wastes generated from PCB manufacturing process are shown in Figure 1.6. From the figure it is concluded that the hazardous wastes accounted about 80% of the total waste generated, of which the liquid waste slurry, solid wastes edge trim and waste board covered 52%, 12%, and 8%, respectively.

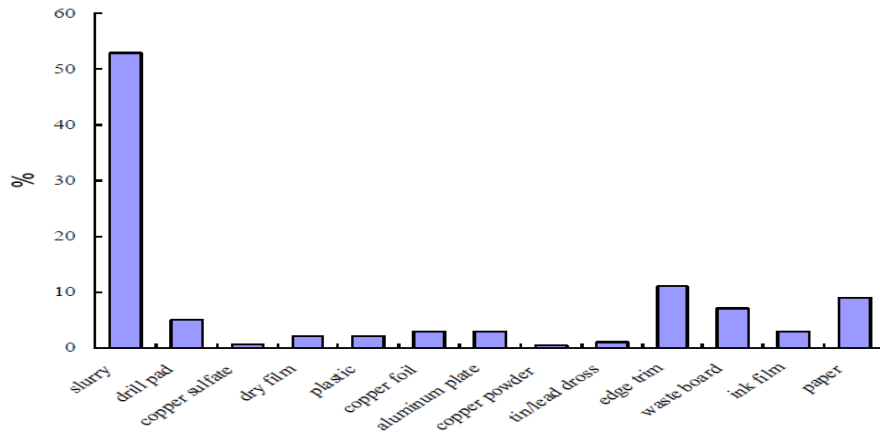


Figure 1.6. Proportions of wastes generated from PCB manufacturing in Taiwan [47].

1.3.1.5. Waste PCBs and the environment

The PCBs industry causes a serious problem due to its waste consists of a lot of hazardous materials like BFRs, Poly Vinyl Chloride (PVC) and toxic metals. In addition, burning of waste PCBs results in the production new toxic substances like dioxins, furans and Polycyclic Aromatic Hydrocarbons (PAHs) which are very dangerous for health and environment [49]. Furthermore, the environment near waste PCBs processing places are more contaminated by the above toxic substances than other sites. According to the Basel Action Network (BAN) report in China, the sample taken from the Lianjiang river near to the recycling area of waste PCBs showed its lead contents is much higher than WHO drinking water limit [50].

The percentages of substances emitted into the air and water bodies from U.S. PCBs industries in 2006 are shown by Figure 1.7. The largest amounts of substances emitted into the air were ammonia, glycol ethers, and dimethylformamide, whereas the chemicals released into water were methanol, copper and its compounds, and formaldehyde [21].

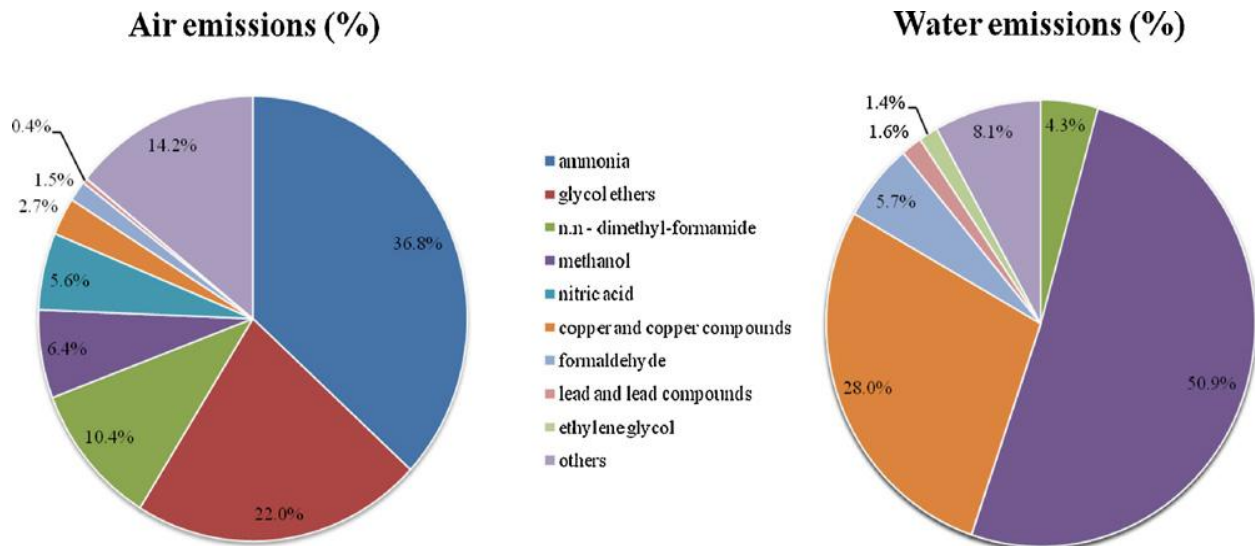


Figure 1.7. Air and water emission percent of chemicals in 2006 from the US PCB industry [21].

1.4. Chemical Etching

Chemical etching is the ancient non-traditional technical process used for the production of complicated machines. It is also called as etching or chemical machining. The process needs chemical known as etchant to discard unnecessary materials. Etching is the process that can be applied to all engineering materials and electronics manufacturers [51].

It is the oldest process used by ancient Egyptians for etching of copper with citric acid for the production of jewelry before 2500B.C. The technique substituted hand-tool design in the 15th century; when weapons and metallic hats were made by using mineral acids. Etching was used for production of steel parts for the first time in 17th century. The development of chemistry resulted in the advancement of etching and different etching chemicals were produced in 18th and 19th centuries [52].

Major advancements of etching were observed after the Second World War and it has been commonly used as industrial process since 1950s. It was first used in USA Aviation, to etch aluminium parts for rockets and remove overweight from aircraft parts. The development of the technique brought the application of etching for different industrial, medical and decorative purposes. In contrast with the traditional machining processes, etching has more advantages because it doesn't need special materials, it needs short machining time, it requires less economy and it provides complex geometrical designs with better precision [53].

1.4.1. Copper etchants in PCB manufacturing

The good electricity transmitting property of copper make it highly used in different electronics and automotive industries [54]. Copper etching is one of the major steps in PCB manufacturing processes. In PCB production, the uncoated copper is dissolved into the etchant to bring the required circuit shape. About 70% of the copper layer is etched by the etching chemical, showing that a large amount of copper containing spent etchant is produced. As the etching process continues and the copper amount in the solution becomes high, the rate of etching slowly decreases and the etching solution should be replaced with new etchant [55].

In etching steps, the components of the layer needed for the desired applications are covered by etch resist to protect them being affected etchants. There are two kinds of resists commonly used in PCBs processes. These are organic and metallic resists. Organic resists are also called as photoresists and they are prepared from organic chemicals. These types of resists are used during the etching of inner layers. Whereas, metallic resists are prepared from pure metals and they are used when outer layers are etched [56]. The general etching process involved in PCBs manufacture can be showed by Figure 1.8 [57].

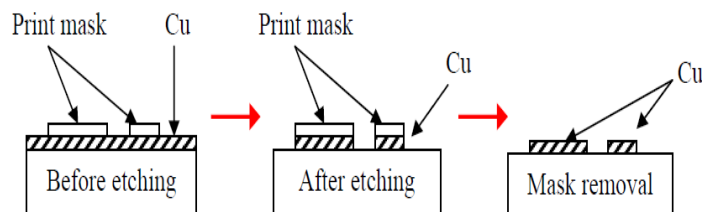


Figure 1.8. A general etching process to remove unwanted copper from PCBs board.

Different etching solutions are used for copper etching. However, their uses depend on their etching rate, dissolving capacity of copper and regeneration of waste etchant. The three most commonly used etchants for copper etching in PCB industries are ferric chloride (FeCl_3), cupric chloride (CuCl_2), and alkaline (ammoniacal) etchants [58].

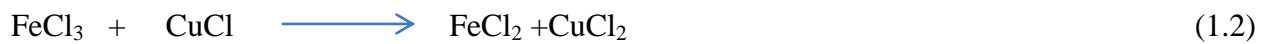
1.4.1.1. Ferric chloride (FeCl_3) etchant

Ferric chloride is the first etchant in PCB industry. It has been applied since the mid of 20th century [59]. FeCl_3 is a common etchant for metals and their alloys. The maximum copper

dissolving capacity of FeCl₃ is 120 g/L. A lot of copper etching studies were done by using FeCl₃ etchant with better etching results. The main problem of this etchant that limits its application is the impossibility of the regeneration of the etchant. Its reaction with copper in etching process is shown below [60].



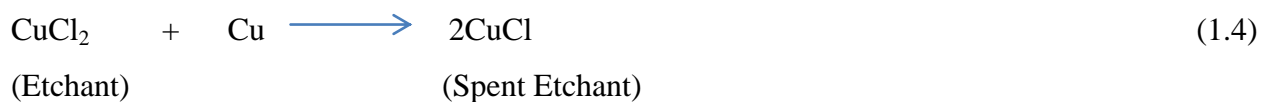
Copper reacts with ferric ions, producing cuprous chloride (CuCl) and ferrous chloride (FeCl₂). CuCl reacts again with FeCl₃ to give CuCl₂. The CuCl₂ finally reacts with copper to produce CuCl as shown in equations 1.2 and 1.3:



1.4.1.2. Cupric chloride (CuCl₂) etchant

Cupric chloride has been used as copper etchant in the PCB industry since 1960s [61]. It is a common etchant for the production of single-sided PCBs and has the advantage of high etching rate than FeCl₃ [62]. Its maximum dissolving capacity is 150 g/L and it doesn't produce sludge as FeCl₃ does [63]. In addition, its regeneration behavior makes it more preferable etchant than FeCl₃. Like FeCl₃ etchant, CuCl₂ is also used for etching of copper alloys such as brass, bronze, etc [62].

In cupric chloride etching, the reaction between copper and CuCl₂ etchant brings the formation of cuprous chloride as seen in equation 1.4. Here, copper is etched by the solution of itself because the oxidation state of copper can be changed from one to another [64]



The two major factors influencing copper etching process using CuCl₂ etchant are molarity and temperature. The molarity of cupric chloride etchant is represented by Baumé. The average Baumé value for good etching rate is 32-33 °Bé (2.33-2.5 Mol) [65]. The other factor that influences the process of etching is temperature. The study showed that the rate of etching increases with increasing temperature. The average etching temperature is around 50°C [66].

The process of alkaline etchants is affected by pH, copper concentration, chloride content and temperature. All these factors should be considered properly to get the best etching process. Despite alkaline etchant is the most commonly used etchant in most PCB industry, it has some drawbacks. Its advantages and limitations are mentioned below [68].

Advantages of using alkaline etchant

- It is widely used for most metallic resists.
- It has relatively high etching rate.
- It has less environmental problems

Disadvantages of using alkaline etchant

- Low viscosity enhances chemistry migration.
- Crystallizes result in material problems
- It results in bad ammonia odor.
- Formation of hazardous waste complex between copper and ammonia

1.5. Spent Etchant

The PCB industry results in the production of toxic effluents which have environmental and public health effects. Spent etchant is one of the hazardous waste solution generated from the etching step in PCB manufacturing process [8]. The most common spent etchant solution produced in PCB industries is ammoniacal spent etchant. This solution is generated when copper is etched with alkaline etchants. Its pH is mostly in the range between 8.5-9.5. The concentrations of copper, chloride, and ammonia in ammoniacal spent etchant are 130-160g/L, 175-190g/L, and 170-201g/L, respectively with molar ratio of ammonia to copper 4:1 [14]. As indicated in Table 1.2, the solution also contains additional chemicals needed for the etching process.

The amount of produced spent etchant is increasing as a result of the growth of PCB manufacturers. According to Mac Dermid's study in 2002, about 70,000L alkaline spent etchant is generated monthly by Singapore's PCB industry [70]. Moreover, the research conducted in china in 2009 indicated that the amount of spent ammoniacal etchant that can be produced every day by PCB industries is around 600 tons [71]. This spent etchant is commonly stored in containers and are finally moved to treatment plants for copper recovery before discharging. Transportation

and final discharging of the spent etchant cause environmental and health risks [72]. Therefore, it is necessary to take precaution during transportation and know the discharging limit before disposal.

Table 1.2. Contents of spent ammoniacal (alkaline) etchant wastewater [73].

pH	10
Cu(II) (M)	2.5
Total NH ₃ (M)	10
Cl ⁻ (M)	5
Na ⁺ (M)	2.5×10^{-2}
Zn (II) (M)	1.7×10^{-3}
Hg (II) (M)	4.7×10^{-4}
Ni (II) (M)	3.4×10^{-4}
Ca (II) (M)	9.3×10^{-5}
Total Fe (M)	4.7×10^{-5}
Cd (II) (M)	1.8×10^{-6}

1.5.1. Environmental and health impacts of spent etchant

Major contents of the spent etchant solution are ammonia, copper, and other heavy metals that have health and environmental impacts if they are not disposed according to their disposal limits. Ammonia is a major pollutant in wastewaters and its amounts in municipal and industrial wastewaters are 10-200 mg/L and 5-1000 mg/L, respectively [74].

The most difficult environmental and health problem of spent etchant is caused by the formation of complex between ammonia and copper. With certain metals (such as nickel and copper) ammonia forms complexes which are very difficult to break and; therefore, prevent the precipitation of the metals. $[\text{Cu}(\text{NH}_3)_4]^{2+}$ is the major complex specie formed in spent ammoniacal etchant [15]. The presence of copper and ammonia make it to be characterized as hazardous waste which needs treatment before discharging into the environment. Besides, from the economical point of view, the high content of copper it contains makes it a valuable waste solution due to the possibility of recovery of copper [47].

1.6. Copper in Wastewaters

The effect of heavy metals on the environment and public health is becoming the most serious problems nowadays [75]. At least half of the 20 known toxic metals are emitted into the environment from various industries and cause complicated problems [76]

Copper is one of the metals existing in the environment and is important for proper growth [77]. However, both excess and deficient of copper cause various problems both in plants and animals [78]. For example, the normal Copper amount in plants is 4–15 mg/kg and its concentration greater than 25 mg/kg is toxic to them [79]. Shortage of copper leads to reduction of cell functions. In contrast, excess of copper destroys plasma membrane and leads to the death of plants [80].

In the case of humans, excessive ingestion of copper in human diet causes cramps, vomit and even death. Whereas, its shortage results in anemia, diarrhea, and nervous disturbances [81]. Besides, if copper's concentration in drinking water is beyond the permissible limit, it damages central nervous system, capillary, renal and kidney [82]. Furthermore, the activities of some enzymes can be inhibited by high Cu^{2+} ion concentrations [83]. Likewise, excessive intake of copper is also harmful to aquatic environment [84]. For this reason, it is important to remove this metal from aqueous solutions before its disposal into the environment.

1.6.1. Copper removal methods from wastewaters

Copper can be removed from different waste effluents using chemical precipitation, ion exchange, membrane filtration, etc [16]. However, these conventional methods have their own limitations such as production of large volume of sludge in case of chemical precipitation [85]. Therefore, it is necessary to find economic copper removal methods.

Currently, neutralization and solvent extraction are the two methods widely used in PCB industries for copper removal. In neutralization, the combination of acid-base and alkaline-base spent etchants results in the formation of $\text{Cu}(\text{OH})_2$, which is broken down to CuO by heating. The limitations of these methods are the produced waste water needs further treatment of copper and the treated spent etchant is not re-usable.

Nowadays, the Mecer® system is becoming one of the successful methods for spent etchant treatment. This method uses solvent extraction and incorporates organic extracts, which extract copper from spent etchant. The reusability of the treated etchant after the removal of copper makes the method economical [86]. Like the other methods, this method has also some limitations such as it needs high cost [87]. Therefore, it is necessary to find a more efficient, an easy to control and low cost technologies.

Based on these, adsorption using nanoparticles is nowadays becoming an attraction method for copper removal and other heavy metals from different aqueous solutions. Especially, using magnetic nanoparticles gives an extra advantage over other nanoparticle adsorbents due to their magnetic characteristics [88].

1.7. Magnetic Nanoparticles (MNPs)

Magnetic nanoparticles are part of nanoparticles that show a response during the application of magnetic field. Nanoparticle (NP) materials have usually core diameter 1-100 nm [89] and those with core diameter less than 20-30nm show super-magnetic behavior [90]. It is normally impossible to separate adsorbents from solution, but magnetic nanoparticles can do it because of their magnetic behavior [91]. The magnetic characteristics of MNPs result in their wide applications for solving a lot of health and environmental problems [92]. Particularly, the low toxicity effect of iron (Fe) over other NPs makes it attractive in different areas.

1.7.1. Applications of iron oxide nanoparticles

Magnetite (Fe_3O_4) is the main type of iron oxide and it is black in color. The ferrimagnetic mineral contains Fe^{II} and Fe^{III} [93]. Using of iron oxide nanoparticles (IONPs) is becoming more common in different areas because of its special characteristics like small size, magnetic behavior and less toxic. The two major application areas of IONPs are in medicine and environmental remediation [94]. The following section provides a short introduction to these two application areas.

1.7.1.1. Medical application of IONPs

Due to their superparamagnetic properties and relatively low harmful effects, the use of IONPs in several medical applications is higher than other magnetic nanoparticles [95]. One of the most in medical area is its application in magnetic resonance imaging (MRI) [96]. IONPs are less toxic and increase the contrast in some MRI applications. They are able to move the blood-brain membrane and stay there for long days [97], which give the advantages for investigation of brain tumors without renewal of the contrast agent [98]. The supermagnetic characteristics of IONP has also direct medical advantages in such way that they can directly be injected into the tumor which induces hyperthermia of the surrounding tumor tissue [99].

1.7.1.2. Environmental applications of IONPs

One of the most environmental applications of IONP is for ground water remediation. The nanoparticle is directly injected into groundwater to remove the pollutants as seen in Figure 1.9. Their high surface area enable them provide large reactivity in respect to granular materials [100]. This property of IONP is very important to conserve both raw materials and energy with significant associated cost savings. Based on the nature of the pollutants, wide range of contaminants including organic compounds, chlorinated pesticides, nitroamines and heavy metals can effectively be removed using IONP [101]. Due to its high reactivity behavior, nanoscale zerovalent iron (Fe^0/nZVI) is commonly used for the purpose of ground water remediation [102]. It is reported that the reactivity of nanoscale zerovalent iron was 10 – 1,000 times higher than granular iron [103].

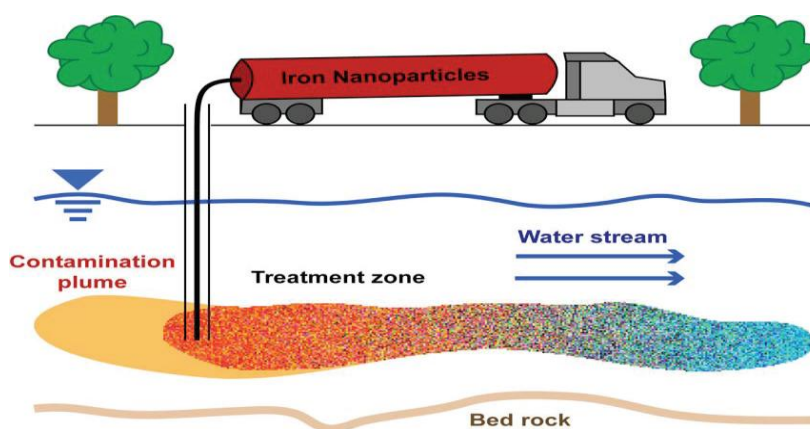


Figure 1.9. Simplified scheme of the utilization of IONP for polluted groundwater remediation

1.7.2. Surface coating (modification) of nanoparticles

To increase the adsorption efficiency, the produced nanoparticle is coated by different substances. The surface coating can be achieved using inorganic substances or polymers. These coating layers have two advantages for the iron core. These are protecting the nanoparticles in solution and help the iron oxide nanoparticles binding to the various functional groups [104]. The functional groups are mostly negatively charged that have the ability to adsorb metals on their surfaces. Some of the major functional groups used for binding metals on the surface of nanoparticles are hydroxyl, carboxyl, amine and amide [105].

1.7.3. Removal of Cu^{2+} ions from wastewaters using surface coated MNPs

Copper can be removed from different water streams by the use of metal oxide magnetic nanoparticles [91]. According to different studies, the use of surface coated iron oxide magnetic nanoparticles is becoming common method for copper removal from various water media [106]. The results indicated that surface modified MNPs effectively remove Cu^{2+} ions from wastewater better than the uncoated ones [107]. This is because the coated MNPs are protected from agglomeration and as a result more stabilized and homogeneous solutions are obtained [20]. However, atleast two steps are required to prepare the modified MNPs; these are preparation of the magnetic cores and coating with polymers [108]. The Schematic model of surface coating of iron oxide is shown below.

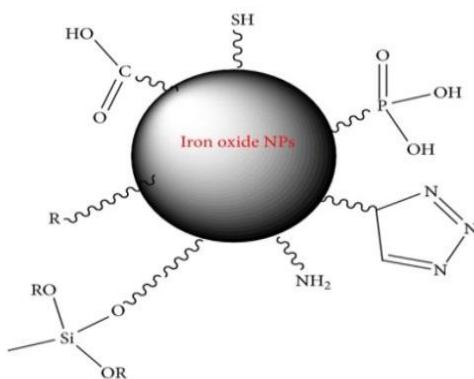


Figure 1.10. Schematic model of surface modification of iron oxide [109].

In our study, chitosan, PVP, oleic acid and PVA were used as coating polymers of iron oxide MNPs and their adsorption capacities in removing Cu^{2+} ions from alkaline spent etchant solution

were compared with the bare iron oxide MNPs. The structure of Fe₃O₄ and the organic polymers used to coat the iron nanoparticle in this study are shown below 1.11.

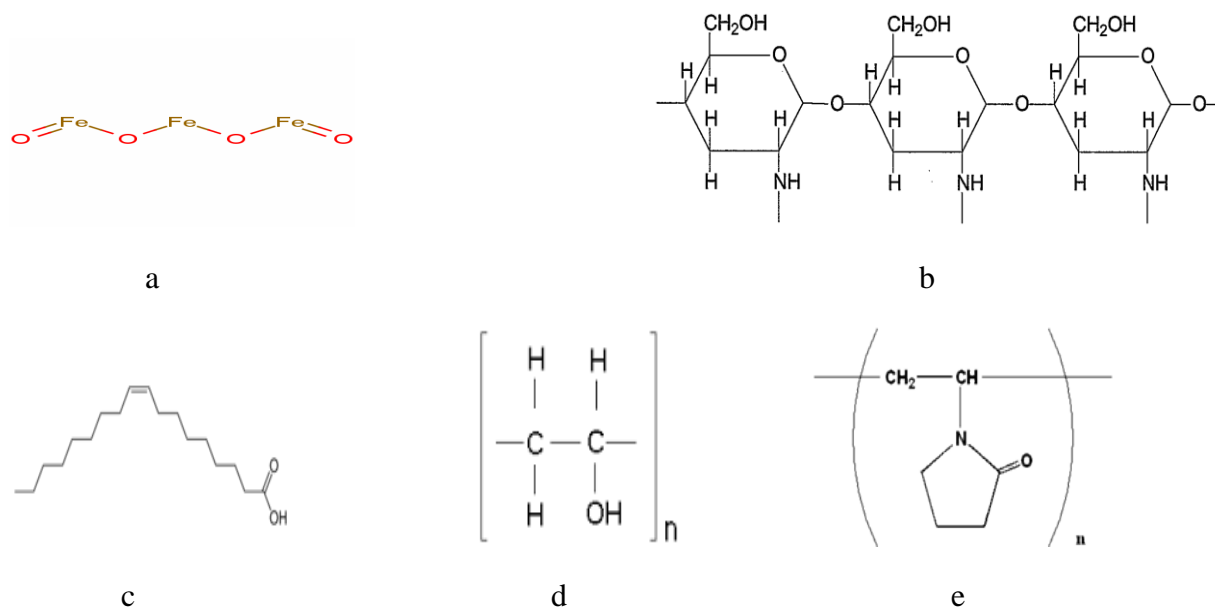


Figure 1.11. Chemical structures: (a) Fe₃O₄ ; (b) Chitosan; (c) Oleic Acid; (d) PVA; (e) PVP

1.7.4. Important properties of magnetic nanoparticles

1.7.4.1. Crystallite size

One of the determining factors for the proper application of magnetic nanoparticles is crystallite size. Due to its influence on the properties of materials, crystallite size has a great position in studying nanomaterials. Size of particles influences the electronic characteristics of substances [110]. The particle size of nanomaterials is given by Debye Scherrer equation:

$$t = \frac{0.9\lambda}{B \cos \theta} \quad (1.7)$$

Where, t size, λ is wavelength, β corresponds to the full width at half maximum intensity (fwhm, in radians), and θ is the Bragg angle.

1.7.4.2. Zeta potential

Zeta potential (ζ) indicates the attraction and repulsion ability of the particles at the surface and it explains the stability of particles. If a particle stays in suspension and does not coagulate, it

is said stable. The stability of particles is determined by the forces of attraction and repulsion. The diagram below shows how ions are distributed around a charged particle.

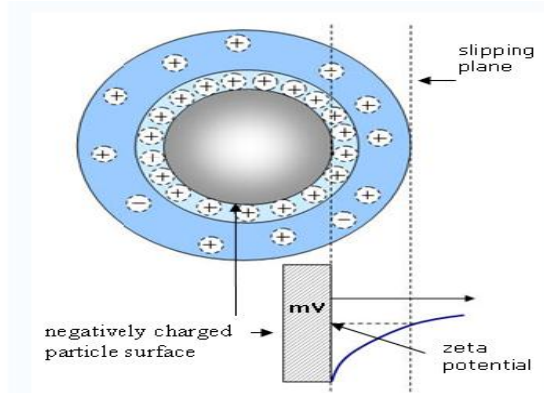


Figure 1.12. Illustration for ions distributed around a charged particle

The causes of attraction and repulsion forces are Van der Waals and electrostatic forces, respectively and they are indirectly measured by Zeta potential, which is calculated as:

$$\xi = \frac{4\pi qd}{D} \quad (1.8)$$

ξ : Zeta potential

q: Charge per unit area

d: thickness of the layer

D: Dielectric constant of liquid.

The major factor that affects zeta potential according to the above equation is the thickness of the layer (d). Greater zeta potential has greater repulsion forces and vice versa. The following diagram shows interparticle potential versus interparticle distance of a particle [111].

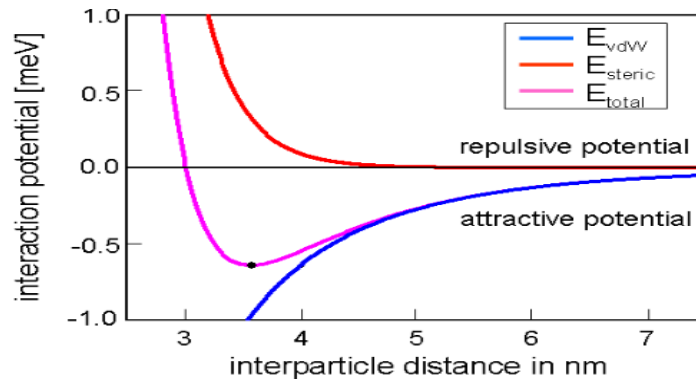
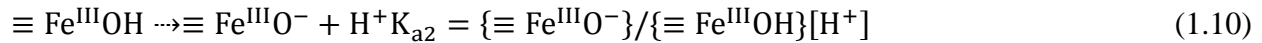
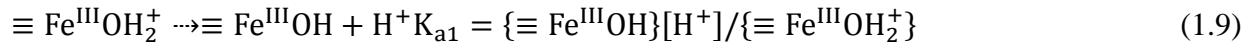


Figure 1.13. Interparticle potential versus interparticle distance of particles.

1.7.4.3. Point of zero charge

Point of zero charge (pzc) represents the pH values where the net surface charge is zero. It shows the surface situation where the surface charge is determined by proton exchange over the surface. For example, if the surface charge is dominated by H^+ , it refers to the point of zero net proton charge. The pH of the point of zero net proton charge of metal oxides is found from electrostatic determinations. The pH of the point of zero net proton charge of a simple oxide is related to the cationic charge and radius of the central ion [112].

In aqueous solution, Fe_3O_4 are surrounded by OH^- . The binding of H^+ and OH^- ions on iron oxide surfaces can be determined by surface coordination reactions at oxide-water interface. The pH-dependent charge of iron oxides results from proton transfers at the amphoteric surface is expressed as follows [113]:



where K is apparent acidity constant, and [] and { } indicate the concentrations of species in the aqueous phase (mole/L) and concentrations of solid species (mole/g), respectively.

At higher pH negative charges, $\{\equiv Fe^{III}O^-\}$, and lower pH, positive charges, $\{\equiv Fe^{III}OH_2^+\}$ are dominant around Fe_3O_4 .

1.7.5. Characterization of magnetic nanoparticles

1.7.5.1. Scanning and transmission electron microscopy (SEM and TEM)

The information about the size, shape and structure of nanomaterials can be given by using microscopic applications. Scanning Electron Microscopy (SEM) and Transmission Electron Microscopy (TEM) are the two common techniques for the characterization of nanomaterials. A common drawback of these techniques is that in some cases particle shape can induce indirect modification of the spectroscopic signal and is thus a source of error in these types of measurements. Nevertheless, both of these techniques are highly used and effective methods for nanoparticles characterization [110].

1.7.5.2. X-ray diffraction (XRD)

This technique was used for studying the order of atomic structure in crystals. Currently, it is used for characterization of nanoparticles. The pattern, position, intensity, and shape of the peaks in XRD are all affected by the atomic structure. XRD is also used in mineralogy to compare the diffraction pattern of samples. Moreover, the size of nanoparticles can also be derived by using XRD pattern because the peak is strongly affected by the particle size [111].

1.7.5.3. Fourier transform infra-red spectroscopy (FTIR)

FTIR technique is the common infrared spectroscopy used in many types of analysis. It shows the image of the sample with its absorption peaks. In FTIR analysis, the infrared radiation is absorbed or transmitted producing fingerprint of the sample. Due to the difference combination of atoms in two different compounds, the two compounds never give identical FTIR results. For this reason, FTIR analysis produces a positive identification for each different types of substance [114].

2. MATERIALS AND METHODS

2.1. Materials

In this study, hydrated copper chloride and ammonia (25%) were used to prepare the synthetic spent etchant solution to simulate the waste effluent generated from the alkaline etching stage of PCB. Whereas, Ferric Chloride hexahydrate (0.5 M), Ferrous Chloride tetrahydrate (0.5 M), and ammonium hydroxide (4M) were used for the preparation of MNP. The brand of the chemicals used in this study was Merck except for ammonium hydroxide which was Vetec brand.

2.2. Methods

2.2.1. Preparation of synthetic spent etchant (Copper stock solution)

The detailed description for preparation of the synthetic spent etchant was as follows: 16.1142 grams of $\text{CuCl}_2 \cdot 2\text{H}_2\text{O}$ and 28.2 mL of NH_3 solution (25%) were mixed in 2L of ultra-pure water. The mixture was stirred by magnetic stirrer for 20-30 minutes at room temperature until it became blue colored, which is the true color of spent ammoniacal etchant. The prepared stock solution is shown in Figure 2.1.



Figure 2.1. The produced synthetic spent etchant (copper stock) solution

2.2.2. Production of magnetite iron oxide (Fe_3O_4) MNP

The production of Fe_3O_4 MNP is clearly described in the following procedures: 20.3g of Ferric Chloride hexahydrate (0.5M, Merck) and 9.94g Ferrous Chloride tetrahydrate (0.5M, Merck) were added into two different beakers containing 150 and 100mL of distilled water, respectively,

and stirred with magnetic stirrer at 250 rpm for 5 minutes. Then, the two solutions were combined and stirred again at 550 rpm for 5 minutes. After that NH_4OH (4M, Vetec) was added until the pH was 9 and the mixture was mixed with mechanical stirrer for 30 minutes. The solution was heated for 20 minutes upto $70\text{ }^\circ\text{C}$ and then cooled to room temperature. After cooling, the MNP was separated using magnetic separation. The separated MNP was washed with distilled water and then ethanol to eliminate any other contaminants. In another experiment, similar solutions were prepared while chitosan, PVP, oleic acid and PVA polymers were added to coat the iron oxide. Finally, the MNPs were put in vacuum dried for 24 hours at $100\text{ }^\circ\text{C}$. The general procedure for the production of MNP is shown in Figure 2.2.

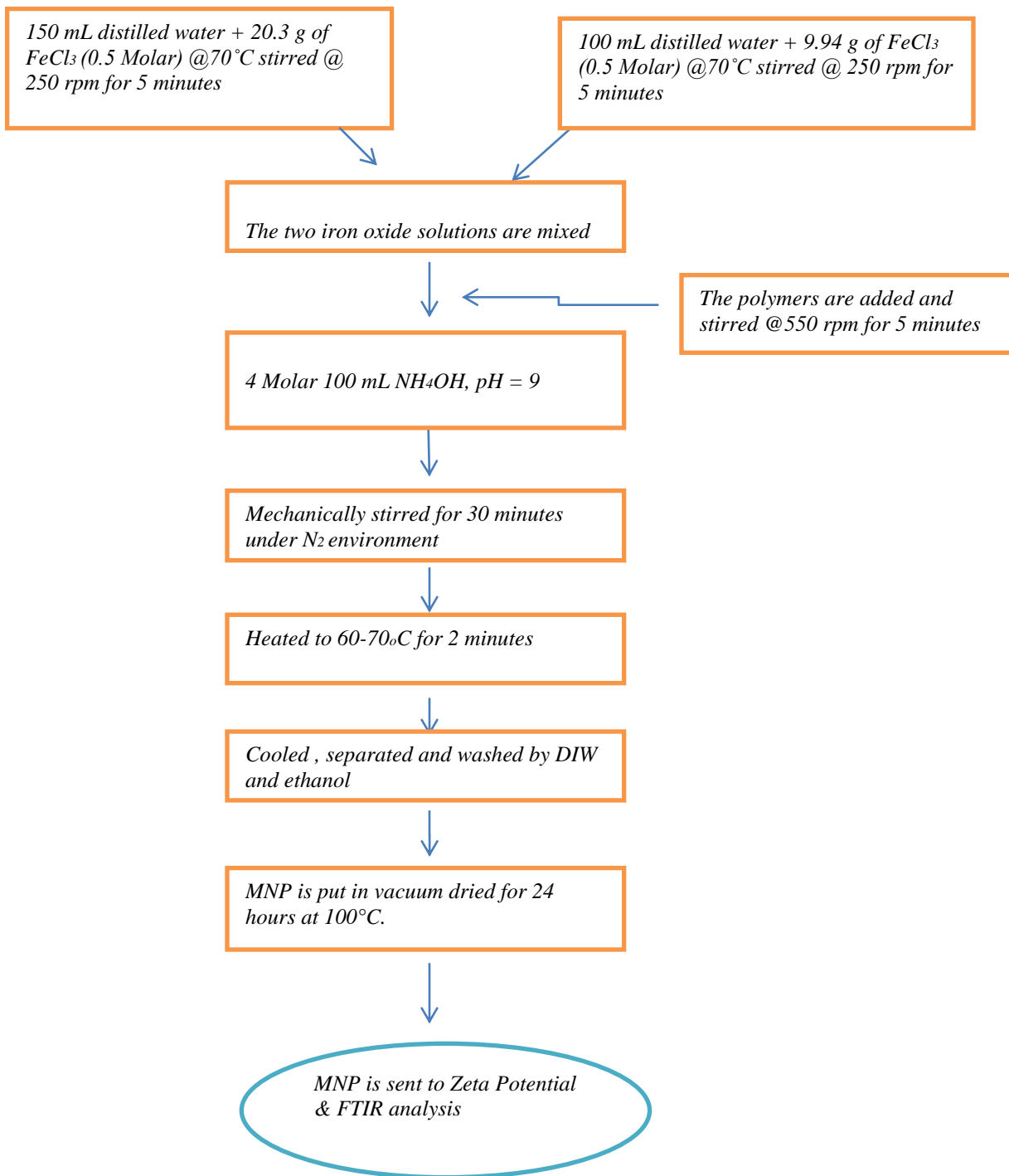


Figure 2.2. Diagram showing MNP production processes [148].

2.2.3. Batch adsorption study

Batch adsorption studies were performed at 20°C in aqueous solutions containing copper (II) ions. For this purpose, 50mL of stock solution was added into flasks containing 0.1, 0.2, 0.3, and 0.4 grams of MNPs. Blank samples were also prepared without the addition of MNP. All flasks were sonicated in ultrasound for 15 minutes to homogenize the mixtures and to prevent natural aggregation. Batch adsorption experiments were conducted using IKA KS 4000 IC control shaker for two hours at 200 rpm and 20°C. The initial and final pH were measured after sonication and shaking, respectively, and found to be between 9.0-9.5. Then, separations of the MNPs were done using magnetic separation technique and the supernatant was collected and filtered with syringes. 2% nitric acid was added to the supernatant to remove any black precipitation. 100µL of supernatant was taken and diluted 500 times for the determination of the remaining concentration of Cu²⁺ ions that were measured using Perkin Elmer AAnalyst 400 Atomic Absorption Spectrometer (AAS). The adsorbed and removed Cu²⁺ ions were determined using the following equations, respectively.

$$q(t) = \frac{(C_0 - C_t)}{m} \times V \quad (2.1)$$

$$\text{Cu(II) removal efficiency (\%)} = \frac{(C_0 - C_t)}{C_0} \times 100 \quad (2.2)$$

Where q (t) (mg/g) is the copper ions adsorbed by unit weight of MNP; C₀ and C_t (mg/L) are initial and final Cu²⁺ ion concentrations, respectively; V (L) is solution volume and m (g) is mass of MNP.

3. RESULTS AND DISCUSSIONS

3.1. Adsorption Studies Results

As explained in section 2.2.3, adsorption studies were carried out in aqueous solutions containing the same Cu^{2+} concentrations (3000 mg/L). Except for the blanks and 0.3 grams of chitosan coated MNP, for each MNP type 0.1, 0.2, 0.3, and 0.4 grams of MNPs were added into each sample flasks as shown in Figure 3.1 (a) and the samples were put in ultrasound bath for 15 minutes (Figure 3.1 (b)). All the samples were subjected to batch adsorption tests conducted using IKA KS 4000 IC control shaker for two hours at 200 rpm and 20°C (Figure 3.1 (c)). Then separation of MNPs were done using magnetic separation technique (Figure 3.1 (d)) and the supernatant was collected and filtered with syringes (Figure 3.1 (e)). Finally 100 μL filtered solutions were taken from each sample and diluted 500 times to bring the final Cu^{2+} concentration to a level that is between the measurable concentration ranges for Atomic Absorption Spectroscopy (AAS). Then, the final Cu^{2+} concentrations were determined by Perkin Elmer AAnalyst 400 Atomic Absorption Spectrometer as shown in (Figure 3.1(f)).

To investigate the details about adsorption, equilibrium studies were carried out at alkaline pH around 9.5 and time conditions needed to reach equilibrium. After copper dosage, the equilibrium adsorbed copper concentration (q_e) as a function of Cu^{2+} concentration (C_e) was plotted in Figure 3.2. As mentioned previously, the MNPs used in this study were chitosan coated, PVP coated, oleic acid coated, PVA coated, lab produced Fe_3O_4 and Aldrich Fe_3O_4 MNPs. The amounts of copper adsorbed by unit weight of MNPs are calculated according to Equation 2.1 and the results are shown in Table 3.1. According to the equation, the highest copper ions adsorbed by unit weight of the above mentioned MNPs were 204.6 mg/g, 189.3 mg/g, 165.3 mg/g, 160.7 mg/g, 23.6 mg/g and 15.4 mg/g, respectively.

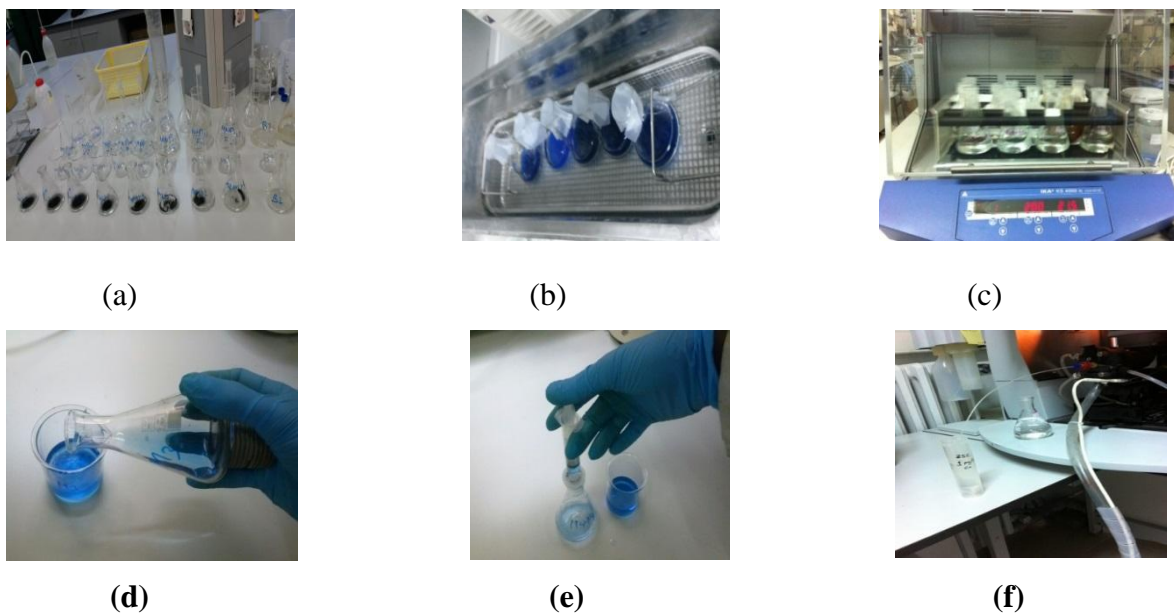


Figure 3.1. Blank and MNP Added Samples (a); Samples in Ultrasound Bath (b); samples in Control Shaker (c); magnetic separation of MNP from solution (d); filtration of the solution using syringe (e); atomic adsorption spectrometer (f).

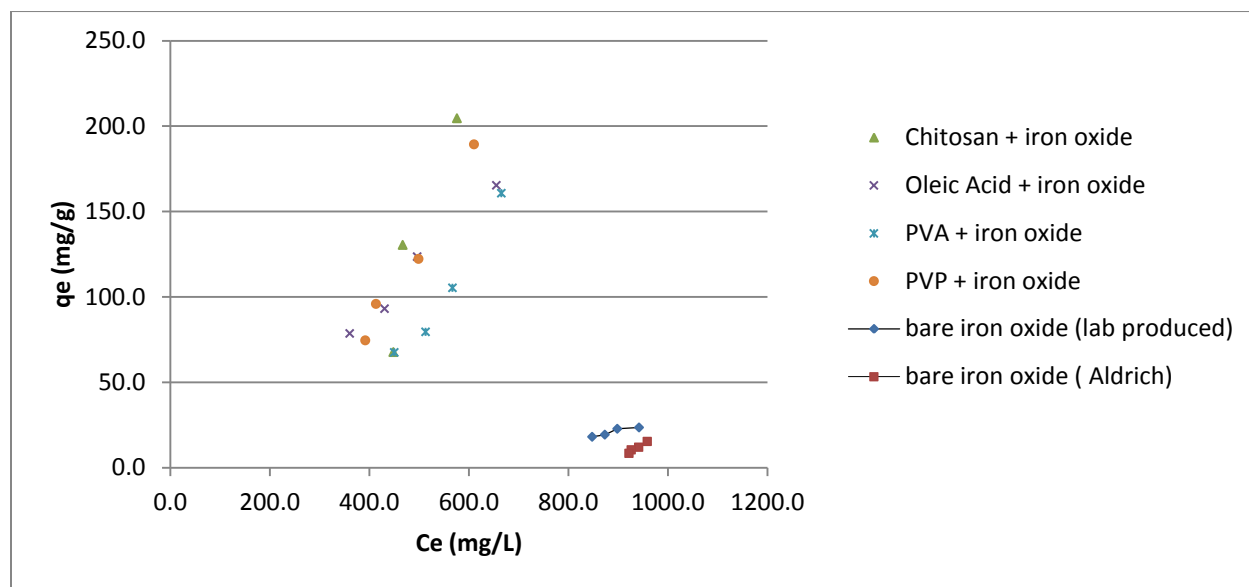


Figure 3.2. C_e versus q_e (initial Cu^{2+} concentration 989 mg/L, time 2 h, pH 9.5, speed 200 rpm, temperature 20°C).

Table 3.1. Results of batch adsorption experiments obtained at 20°C and pH 9.5

Type of MNP	Mass (g)	C _e (mg/l)	q _e (mg/g)
Uncoated Fe ₃ O ₄ (lab. Produced)	0.1	941.75	23.6
	0.2	898	22.8
	0.3	873	19.4
	0.4	847.5	18.1
Uncoated Fe ₃ O ₄ (Aldrich)	0.1	958.3	15.4
	0.2	941	12.0
	0.3	926	10.5
	0.4	921.5	8.4
Chitosan Coated Fe ₃ O ₄	0.1	575.8	204.6
	0.2	466.8	130.4
	0.4	448	67.7
Oleic Acid Coated Fe ₃ O ₄	0.1	655	165.3
	0.2	495.8	123.6
	0.3	430.3	93.1
	0.4	360.3	78.6
PVA Coated Fe ₃ O ₄	0.1	665	160.7
	0.2	566.8	105.3
	0.3	512.8	79.5
	0.4	449.8	67.5
PVP Coated Fe ₃ O ₄	0.1	610	189.3
	0.2	498.5	122.3
	0.3	413	95.9
	0.4	391.5	74.6

Figure 3.2 shows adsorption capacity increases with increasing equilibrium copper ion concentration in solution. The highest copper ions adsorbed was observed by chitosan coated MNP with 204.6 mg/g. This is because the attraction between the negatively charged amine groups of the chitosan and the positively charged copper ions in aqueous solution enable more copper ions adsorption [115]. The value of maximum adsorption capacity (204.6 mg/g) found in this work is higher than many reported results also using amino-functionalized MNPs (~27 mg/g [116]), (~30 mg/g [117]) and (~46 mg/g [118]). Based on the study conducted, chitosan coated MNPs have also high binding affinity to remove various metal ions and bacteria [119]. The general metal adsorption mechanism of metals by chitosan coated Fe₃O₄ MNP is shown by Figure 3.3. The comparison of this study with literature values is given in Table 3.2.

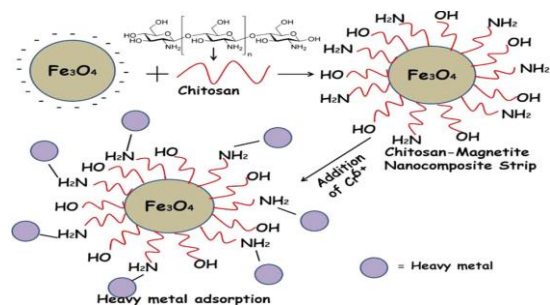


Figure 3.3. Metals adsorption mechanism by chitosan coated MNP [115].

3.1.1. Effect of MNP amount on adsorption

The amount of MNP affects the result of the adsorption study. Therefore, it is highly required to know its amount to increase the binding potential of the targeted metal ions [108]. Figure 3.4 shows the amount of Cu²⁺ ions adsorbed decrease with increasing MNP doses. The decrease in adsorption can be interferences of binding sites and high adsorbent dose which causes low metal ions regarding binding sites [120]. It can also be the reduction of the surface area of the sorbent that is caused by aggregation resulted from high sorbent dose [121]. Furthermore, it may be because of the desorption of the weakly attached metals from the MNP caused by high adsorbent dose in the solution [122]. Therefore, depend on the above discussions, the highest Cu²⁺ ions adsorbed in this study were 204.6 mg/g, 189.3 mg/g, 165.3 mg/g and 160.7 mg/g, 23.6 mg/g and 15.4 mg/g for chitosan coated, PVP coated, oleic acid coated, PVA Coated, lab Fe₃O₄ and Aldrich Fe₃O₄ MNPs, respectively, which were obtained at their lowest MNP dosage (0.1gram).

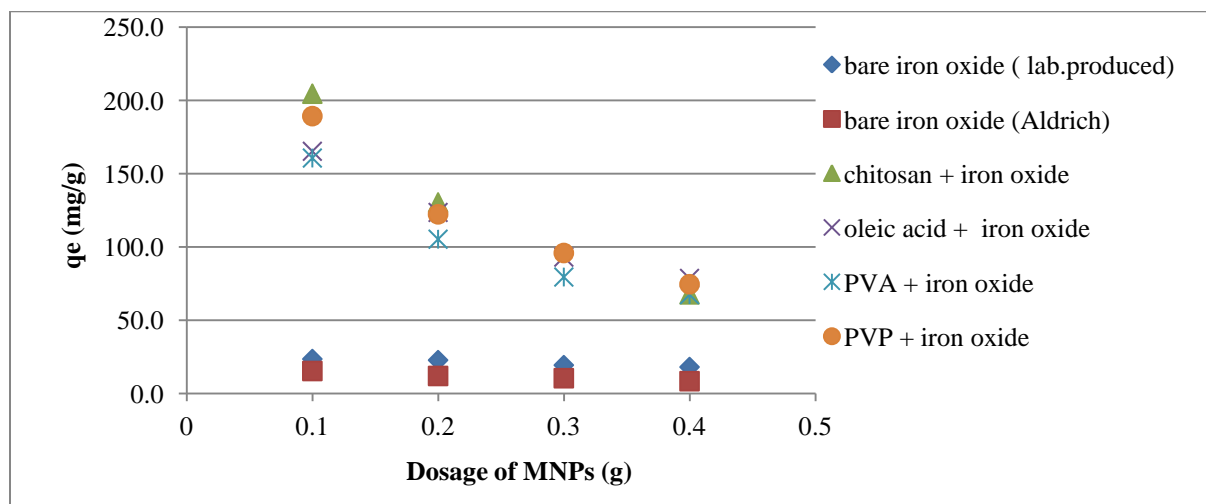


Figure 3.4. Effect of MNPs dosage on the adsorption of Cu²⁺ ions

Table 3.2. Comparison of the results with literature data.

References	MNP used	Coating polymer	Max. Adsorption Capacity (mg/g)	Notes
This study	Fe ₃ O ₄ (Aldrich)	-	15.4	PH = 9.5, Tem.= 20°C, Initial Cu ²⁺ conc.= 989mg/L
	Fe ₃ O ₄ (Lab. Produced)	-	23.6	
		Chitosan	204.6	
		PVP	189.3	
		Oleic Acid	165.3	
	PVA	160.7		
123	Fe ₃ O ₄	1,6-hex- adiazine	25.77	Maximum adsorption occurred at pH 6 and temperature 298 K
124	Fe ₃ O ₄	Humic acid	46.3	Removal efficiency decreased with increasing PH from 2 to 9
125	Maghemite (γ -Fe ₂ O ₃)	-	26.8	Optimum pH was 6.5. The adsorption reached equilibrium within 10 min.
126	Fe ₃ O ₄	Saccharomyces cerevisiae immobilized on chitosan	144.9	Optimum pH was 4.5. Equilibrium achieved in 1 h.
127	Fe ₃ O ₄ microspheres	Poly(acrylic acid) blended chitosan	174	Maximum uptake was at pH 5.5

3.2. Results of Point of Zero Charge

Since the characteristics of the surface charges of polymers and Fe₃O₄ MNPs are not the same, zeta potentials was performed using potentiometric titration method to check the binding of polymers onto Fe₃O₄. For this purpose, 0.03 gram MNPs were dispersed in 600 mL deionized water and titrated to pH 2-10 using 0.1 M HCl or NaOH solution.

Figure 3.5 shows zeta potential of the whole samples increased with the reduction of pH because of the release of H⁺ ions [128]. As a result, higher pH values are preferred for adsorption of Cu²⁺

ions. The result also showed that all MNPs used in adsorption tests had negative surface charges around pH 9.5. This is advantageous in such way that the more negative the surface charge is the higher adsorption capacity to Cu^{2+} ions [129].

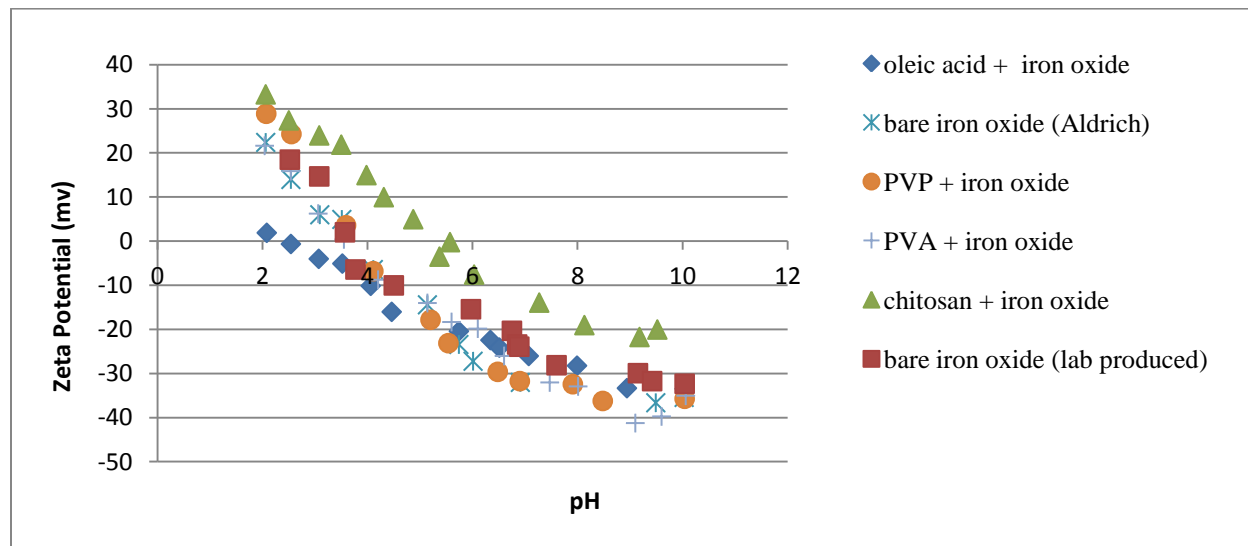


Figure 3.5. Zeta potential of samples at various pH ranges.

Based on the zeta potential results of Figure 3.5, the pH of point of zero charge (pH_{pzc}) of the two pure Fe_3O_4 MNPs was found to be around 3.8, which was lower than the values reported in literatures. In many studies, the average value of pH_{pzc} of pure iron oxide was around 6.5 [130]. The pH_{pzc} of the PVA and PVP coated MNPs also showed almost a similar value with that of the pure iron oxides. But, there were remarkable differences in adsorption capacity of Cu^{2+} ions among them as described in Table 3.1. On the other hand, the pH_{pzc} of the oleic acid and chitosan coated MNPs were found to be around 2.5 and 5.5, respectively. However, in similar with our result, lower pH_{pzc} value for uncoated MNPs than coated MNP was reported in some studies although the coated MNP showed higher adsorption capacity than the uncoated one [131].

Additionally, the figure also shows all the samples had positive zeta potential at pH lower than their respective pH_{pzc} values, this indicates the reaction between the binding sites on the surface of MNPs and the Cu^{2+} ions are repulsive. However, when the pH is higher than pH_{pzc} , the samples had negative zeta potential as a result the attraction between MNPs and Cu^{2+} ions become stronger that results in increasing adsorption [132].

3.3. Results of FTIR Analysis

Magnetic nanoparticles were produced as described in the previous section and characterized by FTIR studies, which is used to investigate distribution of binding groups over the surface of MNPs due to the formation of the interaction between Fe_3O_4 and the polymer shells. For this reason, the FTIR results of the uncoated Fe_3O_4 , pure polymer and polymer coated Fe_3O_4 MNPs were analyzed and discussed below.

Figure 3.6 demonstrates the FTIR spectra of the bare Fe_3O_4 (Fig. 3.6a), pure chitosan (Fig. 3.6b) and chitosan coated Fe_3O_4 MNP (Fig. 3.6c). For the uncoated Fe_3O_4 MNP, the bands at 3213.43 and 1622.84 cm^{-1} are caused by stretching and bending vibrations due to the OH^- groups adsorbed on the surface of iron oxide nanoparticles, respectively [133]. The two distinct absorbent peaks at 543.14 cm^{-1} and 442.94 cm^{-1} belong to the stretching vibration of Fe-O bonds in the octahedral and tetrahedral sites that confirm the formation of Fe_3O_4 MNP [134]. The region between 3200 cm^{-1} to 1630 cm^{-1} is featureless, indicating the sample is free of absorbed water [135]. Due to unavailability of a reference, the researcher could not find the causes of the peaks at 1435.84 cm^{-1} , 1048.09 cm^{-1} and 819.67 cm^{-1} . The FTIR result and explanations for the pure Fe_3O_4 MNP are valid throughout this study.

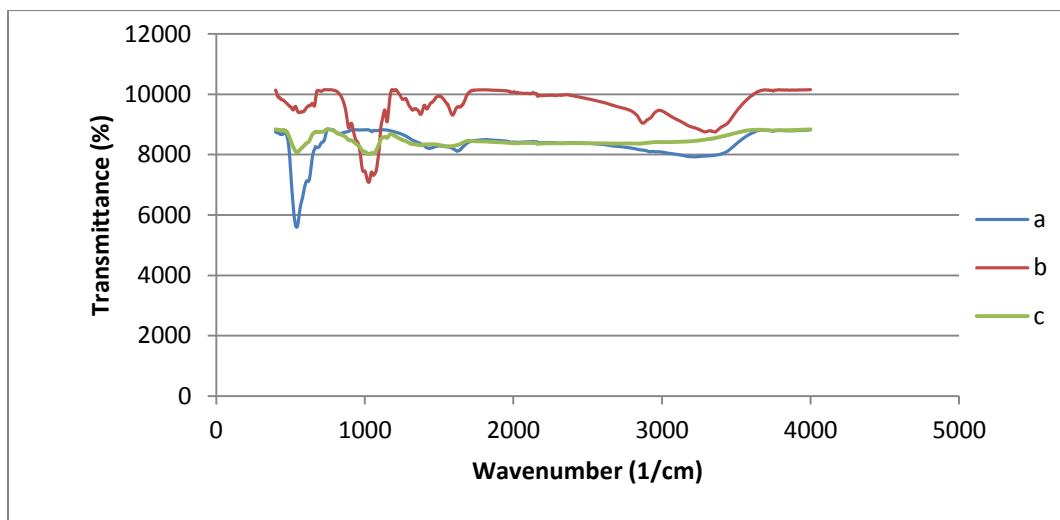


Figure 3.6: FTIR studies of (a) pure Fe_3O_4 ; (b) pure chitosan; (c) chitosan coated Fe_3O_4 MNP

In the case of pure chitosan (Fig. 3.6b), the peaks at 3355.16 cm^{-1} and 2870.99 cm^{-1} are due to stretching vibrations of OH^- and C-H groups, respectively. The peak around 1590.86 cm^{-1}

belongs to bending vibration of N–H (secondary amide). Whereas, the peaks at 1417.65, 1377.90 and 1322.79 cm^{-1} are correspond to CH_3 groups of the polymer [136]. The peaks around 1059.16 and 1026.97 cm^{-1} are caused by stretching vibration of C-O bond. These peaks are also found in the coated sample almost with the same intensities [108].

The FTIR spectrum of chitosan coated Fe_3O_4 MNP is appeared in Figure 3.6c. The peak at 2845.49 cm^{-1} is attributed to C-H bond of methylene group of chitosan. The absorption bands appeared at 1572.55 and 1370.02 cm^{-1} correspond to N–H and C-N bending and stretching vibrations, respectively. The absorption peaks at 547.23 and 455.11 cm^{-1} are resulted from Fe–O group which shows that chitosan was coated on Fe_3O_4 MNP effectively [137]. In this spectrum, the highest absorption peak observed at 3746.92 cm^{-1} varied from the reported value, and the researcher suggested it might be caused by the stretching vibration of OH^- group. Table 3.3 summarizes the FTIR results of pure iron oxide, chitosan and chitosan coated iron oxide.

Table 3.3. FTIR spectra of pure iron oxide, chitosan, and chitosan coated iron oxide

Description	band (1/cm)	Groups
Bare Fe_3O_4	3213.43	*v (OH-)
	1622.84	**δ (OH-)
	543.14	v (Fe–O)
	442.94	v (Fe–O)
	1435, 1048	Unknown
Pure chitosan	3355.16	v (OH-)
	2870.99	v (C-H)
	1590.86	δ (N-H)
	1417.65	CH_3
	1377.9	CH_3
	1322.79	CH_3
Chitosan coated Fe_3O_4	2845.49	C-H
	1572.55	δ (N-H)
	1370.02	v (C-N)
	547, 455	(Fe–O)

*v indicates stretching vibration and **δ indicates bending vibration

In another study, it was reported that the peak at 1150 cm^{-1} (Fig 3.6b) which is caused by vibration of motion of C-O-C group in pure chitosan [138] shifted to around 1058 cm^{-1} in the coated sample, and relatively high amide absorptions were observed in the chitosan coated Fe_3O_4 MNP than in the pure chitosan. This indicates the presence of a strong hydrogen bond between the oxygen atom of iron oxide and the hydrogen atom of the amino group ($-\text{NH}_2$) of the chitosan. This makes sure that it is the amino group not the hydroxyl group ($-\text{OH}$) that is necessary for the binding of chitosan on Fe_3O_4 particle as shown in Figure 3.7 [139].

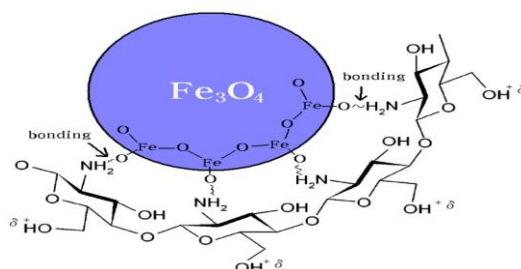


Figure 3.7. Reaction between NH_2 group chitosan and Fe_3O_4 [139].

FTIR analysis of uncoated Fe_3O_4 , pure oleic acid and oleic acid coated Fe_3O_4 MNP is shown in Figure 3.8. The FTIR analysis of the pure Fe_3O_4 has been already discussed above. Here, the FTIR study of the pure oleic acid and oleic acid coated Fe_3O_4 MNP are discussed. In the case of the first (Fig. 3.8b), the bands around 2922.72 and 2853.70 cm^{-1} are caused by the asymmetric and symmetric stretching vibration of CH_2 . An absorption band around 1707.93 cm^{-1} belongs to the stretching vibration of carboxyl group. The O-H in-plane and out-of-plane appear around 1457.57 cm^{-1} and 934.24 cm^{-1} , respectively. The characteristic peaks around 1284.28 cm^{-1} corresponds to the bending vibration of C-O [140].

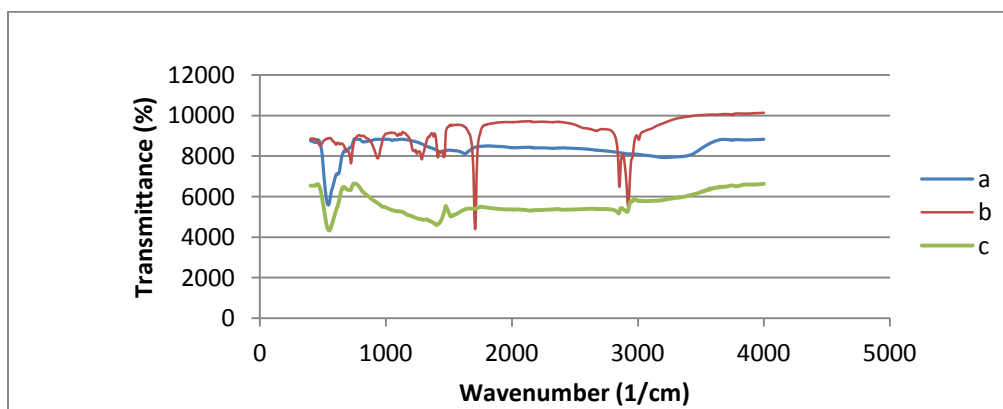


Figure 3.8. FTIR studies of (a) pure Fe_3O_4 ; (b) pure oleic acid; (c) oleic acid coated Fe_3O_4

The FTIR result of oleic acid coated Fe₃O₄ MNP is plotted in Figure 3.8c. Comparing with the study of pure oleic acid, the CH₂ asymmetric and symmetric stretching vibrations shifted to lower frequency regions of 2915.00 and 2846.85 cm⁻¹, respectively. The sharp peak at 1707.93 cm⁻¹ disappeared in Figure 3.8c, but new peak is observed at 1514.99 cm⁻¹ which corresponds to the asymmetric stretching vibrations of C=O group. This assures that binding of oleic acid with Fe atoms of iron oxide takes place by the help of C=O groups of oleic acid as shown in Figure 3.9. There are also characteristic peaks at 1403.09 and 551.14 cm⁻¹ which are due to bending and stretching vibration of C-H and Fe-O bonds, respectively [141]. In the spectrum of the coated sample, the highest peak was observed at 3789.92 cm⁻¹ where the researcher was unable to explain its source because of absence of a reported data. The FTIR spectra of uncoated iron oxide, pure oleic acid, and oleic acid coated iron oxide is summarized in Table 3.4.

Table 3.4. FTIR spectra of pure iron oxide, oleic acid, and oleic acid coated iron oxide

Description	band (1/cm)	Groups
Bare Fe ₃ O ₄	3213.43	v (OH-)
	1622.84	δ (OH-)
	543.14	v (Fe-O)
	442.94	v (Fe-O)
Pure oleic acid	2922.72	V _{as} (CH ₂)
	2853.7	V _s (CH ₂)
	1707.93	v (C=O)
	1457.57	O-H in plane
	934.24	O-H out of plane
	1284.28	δ (C-O)
Oleic acid coated Fe ₃ O ₄	2915	V _{as} (CH ₂)
	2846.85	V _s (CH ₂)
	1514.99	V _{as} (C=O)
	1403.09	δ (C-H)
	551.14	v (Fe-O)



Figure 3.9: bond formation between oleic acid and the iron atom [141].

FTIR analysis of pure iron oxide, pure PVA and PVA coated Fe_3O_4 is displayed in Figure 3.10. The peak at 3273.56 cm^{-1} in the pure PVA (Fig. 3.10b) is resulted from the O-H stretching vibration of the alcohol group in the polymer. However, this band shifted considerably to lower energy (3113.04 and 3007.25 cm^{-1}) for PVA coated iron oxide MNP (Fig. 3.10c). This is the evidence that approves the coating of PVA polymer onto Fe_3O_4 . The absorption bands at 2907.92 and 1658.68 cm^{-1} are attributed to C-H stretching bonding and O-H bending, respectively. The absorbent peaks observed at 1417.54 cm^{-1} and 1325.00 cm^{-1} are from the contributions of CH_2 and C-O-H groups, respectively. The absorbent band at 1088.10 cm^{-1} is resulted from out of phase of C-C-O stretching, whereas the band around 843.66 cm^{-1} is due to C-C skeletal stretching of PVA polymer [142].

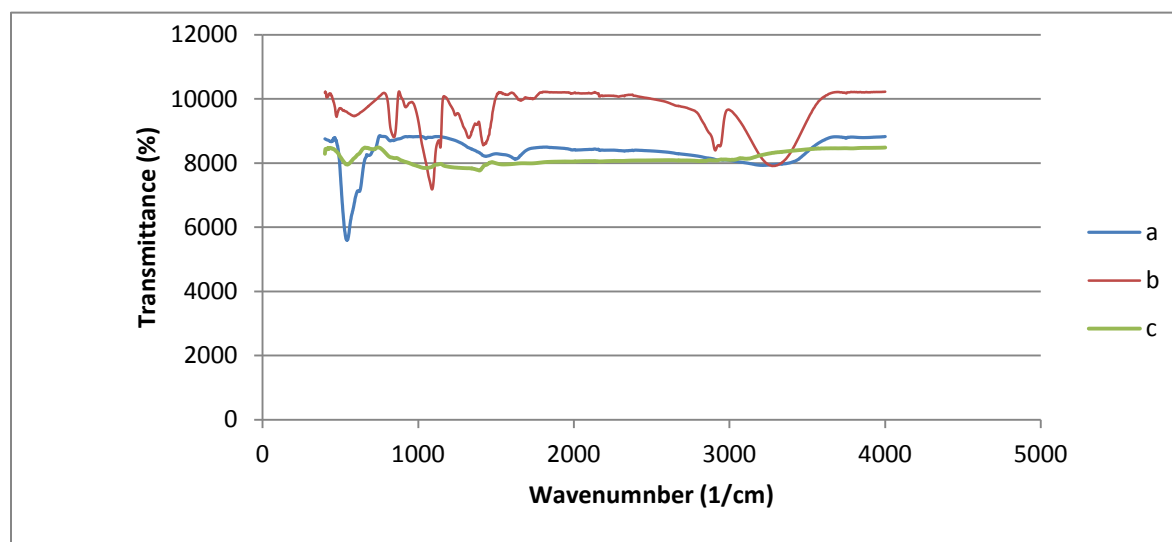


Figure 3.10. FTIR studies of (a) pure Fe_3O_4 ; (b) pure PVA; (c) PVA coated Fe_3O_4

In the case of PVA coated Fe_3O_4 sample (Fig. 3.10c), the adsorption peaks observed at 2913.70 and 2804.89 cm^{-1} belong to the asymmetric CH_2 and symmetric C-H stretching vibration, respectively [143]. The peak at around 1394.19 cm^{-1} is from bending vibration of C-H. Moreover, adsorption band is observed at 1047.63 cm^{-1} which is originated from stretching

vibration of C-O bond [144]. The contribution of metal is shown by the presence of peaks at 1047.63 cm^{-1} in relation with the absorption bands from 543.58 cm^{-1} to 411.28 cm^{-1} , which are attributed to stretching vibration of M-O-C (M=Fe) [143]. The FTIR spectra of uncoated iron oxide, pure PVA, and PVA coated iron oxide is summarized in Table 3.5.

Table 3.5. FTIR spectra of pure iron oxide, pure PVA, and PVA coated iron oxide

Description	band (1/cm)	Groups
Bare Fe ₃ O ₄	3213.43	v (OH-)
	1622.84	δ (OH-)
	543, 442.9	v (Fe-O)
Pure PVA	3273.56	v (OH-)
	2907.92	v (C-H)
	1658.68	δ (OH-)
	1417.54	CH ₂
	1325	C-O-H
	1088.1	V (C-C-O)
	843.66	V (C-C)
PVA coated Fe ₃ O ₄	3113, 3007	v (OH-)
	2913.7	V _{as} (CH ₂)
	2804.89	V _s (CH)
	1394.19	δ (C-H)
	1047.63	V(C-O)
	543, 411	v (Fe-O)

The FTIR results of pure Fe₃O₄, PVP and PVP coated Fe₃O₄ MNP samples are shown in Figure 3.11. According to the result, the peak at 3445.16 cm^{-1} for pure PVP (Fig. 3.11b) is due to stretching vibration of O-H. This peak was shifted to 3212.96 cm^{-1} after coating of PVP on iron oxide MNP (Fig. 3.11c). The absorption peak at 2950.03 cm^{-1} is from asymmetric stretching vibration of C-H group of N-vinyl pyrrolidone. The vibrational bands resulted from the carboxyl group (C=O) shifted from 1659.51 cm^{-1} and 1651.96 cm^{-1} (Fig. 3.11b) to 1622.54 cm^{-1} (Fig. 3.11c) after coating. New absorption peaks appeared for pure PVP in the ranges 1460.65 to 1315.41 cm^{-1} and 1284.16 to 1167.82 cm^{-1} . The peaks in the range 1460.65 and 1315.41 cm^{-1} are attributed to bending vibration of C-H group of N-vinyl pyrrolidone and cyclic deformation of cyclic CH₂. Whereas the peaks in the 1284.16 and 1167.82 cm^{-1} are due to stretching vibration of

C-N and tertiary (3°) amide groups. The absorbent peaks at 546.75 and 435.01 cm^{-1} for PVP coated MNP belong to Fe-O bond. The shifting of the bands are the indications of the interaction between the PVP and Fe ions (Fig.3.11c) [145].

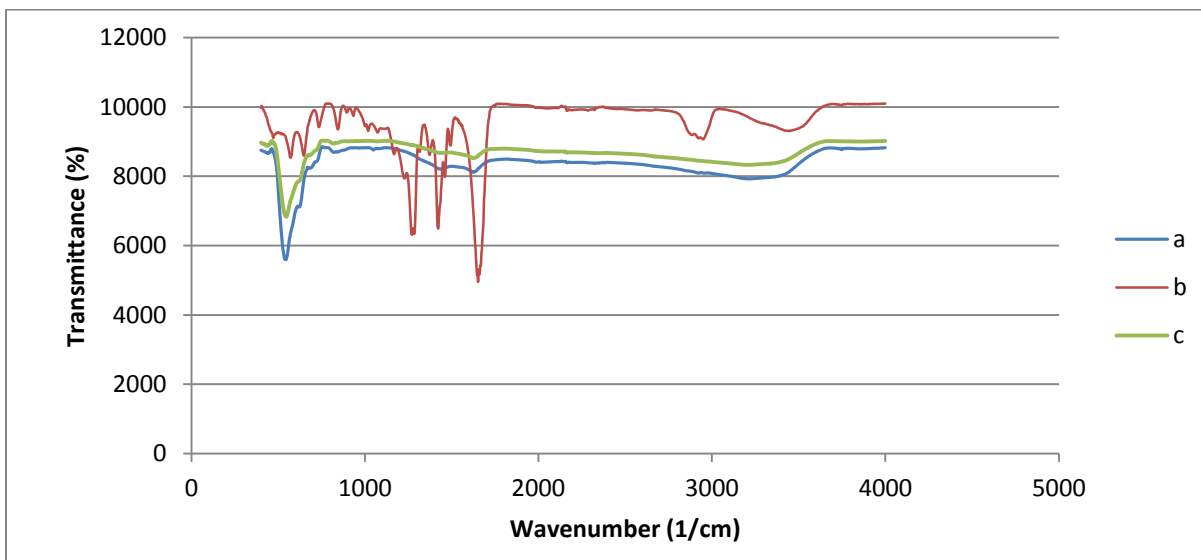


Figure 3.11. FTIR studies of (a) pure Fe_3O_4 ; (b) pure PVP; (c) PVP coated Fe_3O_4

The FTIR spectra of uncoated iron oxide, pure PVP, and PVP coated iron oxide is summarized in Table 3.6.

Table 3.6. FTIR spectra of pure iron oxide, pure PVP, and PVP coated iron oxide

Description	band (1/cm)	Groups
Bare Fe_3O_4	3213.43	ν (OH-)
	1622.84	δ (OH-)
	543, 442.9	ν (Fe-O)
Pure PVP	3445.16	ν (OH-)
	2950.03	ν_{as} (C-H)
	1659, 1651.9	C=O
	1460-1315	δ (C-H)
	1284-1167.8	ν (C-N)
PVP coated Fe_3O_4	3212.96	ν (OH-)
	1622.5	C=O
	546,435	ν (Fe-O)

For the purpose of comparison, the FTIR studies of the two uncoated iron oxide were analyzed and the graphs are shown in Figure 3.12. In the lab produced Fe_3O_4 (Fig. 3.12a), the peaks at 3213.43 and 1622.84 cm^{-1} belong to stretching and bending vibrations of the OH^- groups adsorbed on the surface of Fe_3O_4 MNP, respectively [133]. However, in the Aldrich Fe_3O_4 (Fig. 3.12b), these values shifted to higher peaks of 3789.92 and 1734.64 cm^{-1} , respectively. Moreover, in Figure 3.12a, two peaks were observed at 543.14 cm^{-1} and 442.94 cm^{-1} which correspond to the stretching vibration of Fe–O bonds in the octahedral and tetrahedral sites, respectively [134]. Nevertheless, in the Aldrich MNP, only one peak was observed at 534 cm^{-1} . Furthermore, the absorbent bands around 1435.35 and 1048.09 cm^{-1} (Fig. 3.12a) seem be shifted to 1367.4 and 1074.34 cm^{-1} , respectively (Fig. 3.12b). In addition, new absorbent peaks were observed for the Aldrich MNP in the ranges 2846 and 1735 cm^{-1} . In contrast, this region was featureless for the lab Fe_3O_4 indicating the sample is resistant to uptake of water [135].

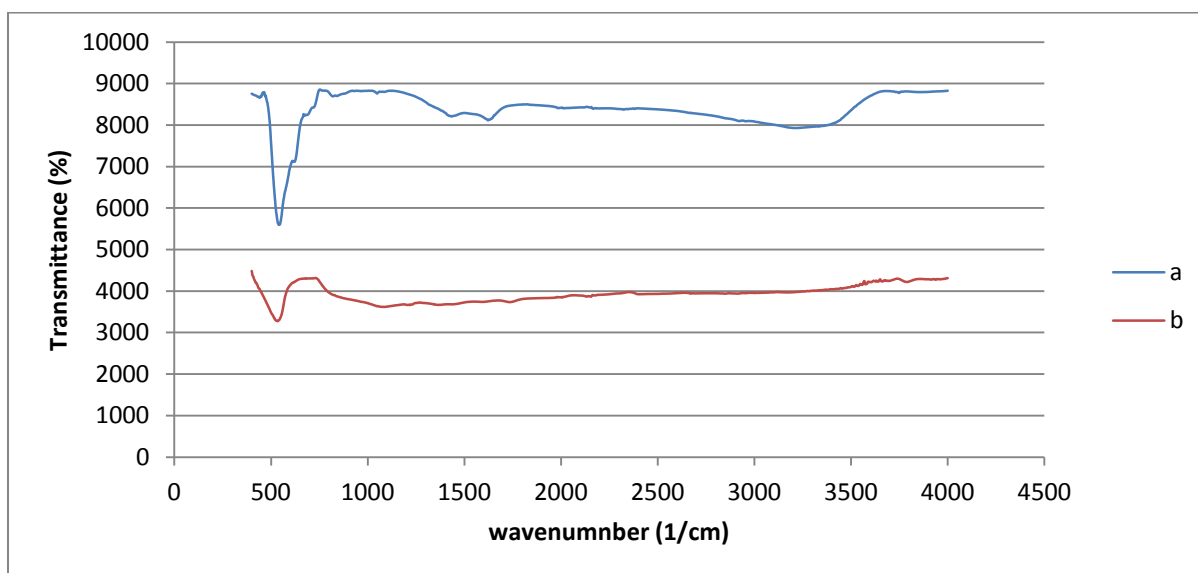


Figure 3.12. FTIR studies of (a) pure Fe_3O_4 (lab Produced); (b) pure Fe_3O_4 (Aldrich)

The FTIR spectra of the laboratorial and commercially produced iron oxide is summarized in Table 3.7.

Table 3.7. FTIR spectra of lab. Produced and Aldrich iron oxide

Description	band (1/cm)	Groups
Lab. Fe ₃ O ₄	3213.43	v (OH-)
	1622.84	δ (OH-)
	543.14, 442.94	v (Fe–O)
	1435, 1048	Unknown
Aldrich Fe ₃ O ₄	3789	May be v (OH-)
	1734	May be δ (OH-)
	534	v (Fe–O)
	2846-1735	Unknown
	1367, 1074	Unknown

3.4. Discussions

Various studies were conducted to treat water streams contaminated with heavy metals using bare and coated MNPs. In this study too, it was tried to compare the adsorption capacities of the bare and various polymer coated MNPs in removing Cu²⁺ ions from wastewater originated from alkaline spent etchant. According to our results, the adsorption capacity of Cu²⁺ ions of the uncoated MNP (lab. Produced Fe₃O₄) was 23.6 mg/g with removal efficiency of 53% (data not shown). Nearly, similar copper adsorption result (26.8 mg/g) was reported by researchers in their study to remove metals from electroplating using uncoated Maghemite (γ-Fe₂O₃) MNP [125]. Additionally, in the result of another study, 15 mg/L and 40.5 mg/L of adsorption of Cu²⁺ ions were achieved from wastewater by the use of bare and coated γ-Fe₂O₃ MNPs, respectively [146].

The results of adsorption are highly affected by the type of polymers used to coat/modify the MNPs. In the research conducted on chitosan-coated MNP, it was reported the adsorption for Cu²⁺ ions were 39 mg/g and 66 mg/g at 18°C and 35 °C, respectively [108]. Besides, the highest adsorption for Cu²⁺ ions obtained using Fe₃O₄ MNP coated with Carboxymethyl-β-cyclodextrin polymer was 47.2mg/g at 25 °C [147]. Nevertheless, high adsorption capacity of copper (maximum 625 mg/g) was also reported using glycine-functionalized γ-Fe₂O₃ MNP (131).

In the case of our study, the highest copper ions adsorbed by unit weight of magnetic nanoparticles were achieved by chitosan and PVP polymer coated MNPs with 204.6 and 189.3

mg/g, respectively. Comparable results were also obtained using oleic acid (165.3 mg/g) and PVA (160.7 mg/g) coated MNPs. In addition, the adsorption result obtained by the bare MNP in our study (23.6 mg/g) was almost similar with even the result obtained using the amino-functionalized MNPs with maximum adsorption capacity of 25.77 mg/g (123). Depending on these results it can be said that our works were not only consistent with literatures but also showed better results than some previous studies.

The researcher tried to find out the possible reasons for the differences in adsorption capacities between this study the reported values, and it is suggested one of the following might be the reason:

1. The type of polymers used for coating MNPs
2. Presence of interferences that compete with the targeted metals for the same binding sites
3. The temperature and pH at which batch adsorption experiment is conducted.
4. The initial Cu^{2+} concentration differences.

Most adsorption experiments are conducted at room temperature. However, in order to obtain the optimum temperature where highest adsorption occurs, some researchers use different adsorption temperatures. In some studies, increasing temperature results in increasing adsorption capacities and vice versa. However, in our study constant temperature (20°C) was used for the all adsorption experiments. For the case of pH, most adsorption studies are carried out at lower or neutral pH. This is because Cu^{2+} ions would precipitate as $\text{Cu}(\text{OH})_2$ at high pH values (132). However, the pH of the waste solution in our study was high (around 9.5). Despite this, high adsorption capacities for Cu^{2+} ions were obtained.

Furthermore, the effect of pH on metal adsorption is also explained in relation with point of zero charge that is obtained from zeta potential analysis. For most adsorption studies, the pH_{pzc} for the bare Fe_3O_4 MNP is in the range 6-7, and shifts to lower value for the coated MNPs. It was also stated at pH higher than pH_{pzc} , the MNP surface is negative and metal adsorption is expected. But, when the pH is lower than pH_{pzc} , metal adsorption is reduced nearly to zero because the MNP surface is positive (132). However it was not true in the case of Copper ions. It was observed at a pH lower than pH_{pzc} , copper ions were still adsorbed onto $\gamma\text{-Fe}_2\text{O}_3$ MNP. This is thought because of ion exchange between Cu^{2+} and H^+ in this pH range [125].

In contrast, the zeta potential results of this study showed the pH_{pzc} values of the bare Fe_3O_4 MNP was found to be around 3.8, which was lower than the reported values and nearly similar to the pH_{pzc} of PVA coated and PVP coated MNPs. The lowest and highest pH_{pzc} values were observed for oleic acid coated and chitosan coated MNPs which were around 2.5 and 5.5, respectively. However, there was still high adsorption of copper ions (165 mg/g) onto the surface of oleic acid coated MNP although it had the lowest pH_{pzc} value.

One of the most important parameters believed to be the reason for the differences in adsorption capacities in various adsorption studies is initial Cu^{2+} concentration. This is related to Chatelier's principles, which states increasing the concentration of a reaction results in increasing the reaction rate because the frequency of successful collisions of the reactants would increase. Based on this principle, when the initial copper concentration of the solution increases, the equilibrium adsorption for the targeted ions also increases. The adsorption study conducted on different initial Cu^{2+} concentration for the removal of Cu^{2+} using amino-functionalized magnetic nanoparticles also showed Cu^{2+} adsorption increased when initial Cu^{2+} ion concentrations of the solution increased [123]. However, in our study, similar initial Cu^{2+} concentration (989 mg/L) was used for the whole experiments.

The FTIR results of our study showed some unique characteristics comparing with the reported values. For example, high adsorption peaks (up to 3750 cm^{-1}) were observed for pure Fe_3O_4 (Aldrich), chitosan coated and oleic acid coated MNPs. Moreover, it was observed that there were also FTIR result differences between the two pure Fe_3O_4 MNPs. The region between $3200\text{--}1630\text{ cm}^{-1}$ in the spectrum of the lab produced Fe_3O_4 MNP was featureless. This indicates that there was no absorption in this region. In contrast, in the case of Aldrich Fe_3O_4 MNP three adsorption peaks were observed in this region. However, the researcher could not find out the exact reason(s) for these variations.

4. CONCLUSIONS

In this paper, the adsorption capacities of the pure and polymer coated Fe₃O₄ MNP in removing Cu²⁺ ions from alkaline spent etchant solution were studied. The polymers used to coat the MNP were chitosan, PVP, PVA and oleic acid. The MNP was produced in Marmara University. The commercial iron oxide MNP (Aldrich) was also used in this study to compare its adsorption capacity with that of the MNP produced in our university.

The results of the adsorption experiment showed that high adsorption of Cu²⁺ ions were observed by the polymer coated MNPs than the uncoated MNPs. The maximum copper adsorptions achieved were 204.6, 189.3, 165.3 and 160.7 mg/g for chitosan, PVP, oleic acid and PVA coated MNPs respectively. The highest adsorption of copper in chitosan coated MNP is due to the strong attraction between amine group of chitosan and Cu²⁺ ions. The lowest copper adsorptions were achieved by the lab produced and Aldrich Fe₃O₄ MNP with highest adsorption capacities of 23.6 and 15.4 mg/g, respectively. The adsorption results of this study were consistent with literature values and better adsorption results were even obtained by some MNP types.

The point of zero charge, which is an important property of MNPs, was also determined by measuring their zeta potentials. According to the result, the uncoated Fe₃O₄ MNPs showed lower pH_{pzc} than the reported values. Zeta potential of the samples decreased when pH increased and the whole MNP types used in this study showed negative zeta potential at higher pH. As a result the surface charges of the MNPs became negative at pH around 9.5. Therefore, higher pH is preferable because it enhances Cu²⁺ ions adsorption on MNP surfaces.

The only MNP characterization methods used in this study was FTIR. Even though some unique characteristic peaks were observed in some samples, all the FTIR results showed the successful attaching of polymers on the surface of Fe₃O₄ MNPs.

In summary, from the results of this study it can be concluded that surface coated MNPs can provide better adsorption results than the uncoated MNPs and can widely be applied for the adsorption studies in removing copper and other heavy metals from water and wastewaters. Finally, the researcher suggests the following directions for future work:

- The present study was conducted in lab-scale operation. It is suggested to develop a continuous adsorption process which will be more suitable for an industrial process.
- Analyze the effects of external factors such as time and temperature on the adsorption processes.
- Conduct desorption experiment to reuse the MNPs again to minimize the cost and time for producing MNPs.
- Conduct experiments using these MNPs to examine their adsorption capacities in removing other heavy metals from water/wastewater.
- This study was conducted on the synthetic wastewater. It is suggested to conduct on the real wastewater.

REFERENCES

- [1] A. Wdjtowicz, A. Stokuosa (2002) Removal of heavy metal ions on smectite ion-exchange column. *Pol. J. Environ. Stud.*, 11 (1), 97–101.
- [2] J. Gao, F. Liu, P. Ling, J. Lei, L. Li, C. Li, A. Li (2013) High efficient removal of Cu (II) by a chelcating resin from strong acidic solutions: Complex formation and DFTcertification. *Chem. Eng. J.*, 222, 240–247.
- [3] Y. Mido, M. Satake (1995) *Chemicals in the Environment*. Discovery Publishing House, New Delhi.
- [4] Y. Pang, G. Zeng, L. Tang, Y. Zhang, Y. Liu, X. Lei, Z. Li, J. Zhang, G. Xie (2011) *Desalination*. 281, 278-284.
- [5] S. Mohan, G. Sreelakshmi (2008) Fixed bed column study for heavy metal removal using phosphate treated rice husk. *J. Hazard. Mater.*, 153, 75–82.
- [6] Y.T. Zhou, H.L. Nie (2009) Removal of Cu (II) from aqueous solution by chitosan-coated magnetic nanoparticles modified with α -ketoglutaric acid. *J. Colloid Interface Sci.*, 330, 29–37.
- [7] ÖZER G, ÖZCAN A, ERDEM B, ÖZCAN A S. (2008) Prediction of the kinetics, equilibrium and thermodynamic parameters of adsorption of copper (II) ions onto 8-hydroxy quinoline immobilized bentonite A: Physicochemical and Engineering Aspects. *J. Colloid and Surfaces Aspects*, 317, 174–185.
- [8] C. F/ Coombs (1988) *Printed Circuits Handbook*,14, McGraw, Hill Book Company.
- [9] LI Jian-guang (2010) Spent acidic etching solution treatment and copper recovery system. *J. Printed Circuit Information* 1, 60-68.
- [10] <http://www.ipc.org/ContentPage.aspx?pageid=IPC-World-PCB-Production-Report-Shows-19-Percent-Growth-in-2010>.
- [11] Q. Yang and N.M. Kocherginsky (2006) *J. Membrane Sci.*, 286, 301.
- [12] Veit HM, Bernardes AM, Ferreira JZ, Tenorio JAS, Malfatti CF. (2006) Recovery of copper from printed circuit boards scraps by mechanical processing and electrometallurgy. *Journal of Hazardous Materials*, 137, 1704–9.
- [13] JIANG Pei-bao, SONG Jiu-chun (1993) *Printed circuit design handbook* (in Chinese), 74-78, China Astronauti Publishing House, Beijing
- [14] W. Schwab and R Kehl (1997) "Copper recycling from spent ammoniacal etching solutions and their regeneration by solvent extraction". *Proceedings of the XX IMPC - Aachen*, 21-26

September, 285-292.

[15] Basolo, F., Pearson, R.G. (1967) *Mechanisms of Inorganic Reactions: A Study of Metal Complexes in Solution*, Wiley, New York.

[16] R.W. Rousseau (Ed.) (1987) *Handbook of Separation Process Technology*, Wiley, New York.

[17] M. Hua, S.J. Zhang, B.C. Pan, W.M. Zhang, L. Lv, Q.X. Zhang (2012) Heavy metal removal from water/wastewater by nano-sized metal oxides: A review. *J. Hazard. Mater.*, 211, 317-331.

[18] S.M. Zhu, N. Yang, D. Zhang (2009) Poly(N,N-dimethylaminoethyl methacrylate) modification of activated carbon for copper ions removal. *Mater. Chem. Phys.*, 113, 784–789.

[19] A.H. Lu, E.L. Salabas, F. Schüth (2007) Magnetic nanoparticles: synthesis, protection, functionalization, and application, *Angew. Chem. Int. Ed.* 46, 1222–1244.

[20] Kraus, A., Jainae, K., Unob, F., Sukpirom (2009) N. Synthesis of MPTS-modified cobalt ferrite nanoparticles and their adsorption properties in relation to Au(III). *J. Colloid Interface Sci.*, 338, 359–365.

[21] M.W. Jawitz (1997) *Printed Circuit Board Materials Handbook*, McGraw-Hill, New York.

[22] NAS (National Academy of Sciences) (2005) *Manufacturing Trends in Electronics Interconnection Technology*. The National Academies Press, Washington, DC Website :(<http://www.books.nap.edu/catalog/11515.html>).

[23] Buckle R, Roy S. (2008) The recovery of copper and tin from waste tin stripping solution Part I: Thermodynamic analysis. *Separation and Purification Technology*, 62, 86–96.

[24] Chi, X., Streicher-Porte, M., Wang, M.Y., Reuter, M.A. (2011b) Informal electronic waste recycling: a sector review with special focus on China *Waste Manage* 31, 731-742 (Oxford).

[25] K.C. Nathsarma, P.V.R.B. Sarma (1993) Processing of ammoniacal solutions containing copper, nickel and cobalt for metal separation, *Hydrometallurgy*, 33 (1–2), 197–210.

[26] Prismark (2012).

[27] WECC Global PCB Production Report for the year 2012.

[28] J. Li, H. Lu, J. Guo, Z. Xu, Y. Zhou (2007) Recycle technology for recovering resources and products from waste printed circuit boards. *Environ. Sci. Technol.*, 41, 1995–2000.

[29] Zhou, Y., Qiu, K. (2010) A new technology for recycling materials from waste printed circuit Boards. *J. Hazard Mater.*, 175, 823-828.

- [30] Hall, W.J., Williams, P.T. (2007b), Separation and recovery of materials from scrap printed circuit boards. *Resour. Conserv. Recy.*, 51, 691-709.
- [31] Sum, E.L. (1991) The recovery of metals from electronic scrap. *JOM*, 43, 53-61.
- [32] Robinson, B. (2009) E-waste: an assessment of global production and environmental impacts. *Sci. Total Environ.*, 408, 183-191.
- [33] Veit, H.M., Bernardes, A.M., Ferreira, J.Z., Tenorio, J.A.S. Malfatti, C.d.F. (2006) Recovery of copper from printed circuit boards scraps by mechanical processing and electrometallurgy. *J. Hazard. Mater.*, 137, 1704-1709.
- [34] La-Dou J. (2006) Printed circuit board industry. *International Journal of Hygiene and Environmental Health*, 209, 211–9.
- [35] Ritchey L.W., Coombs C.F. (2008) Physical characteristics of the PCB. In: Coombs Jr. Clyde F. (Ed.), *Printed Circuits Handbook*, sixth ed. McGraw-Hill.
- [36] J. La Dou (2006) Printed circuit board industry. *Int. J. Hyg. Environ. Health*, 209, 211–219.
- [37] Printed Circuit Board (website: https://www.en.wikipedia.org/.../Printed_circuit_board).
- [38] Environmental Protection Agency (1997a) Design for the environment. (Website: <http://www.epa.gov/dfe/projects/pwb/index.htm>).
- [39] Hunsom M, Pruksathorn K, Damronglerd S, Vergnes H, Duverneuil P. (2005) Electrochemical treatment of heavy metals (Cu^{2+} , Cr^{6+} , Ni^{2+}) from industrial effluent and modeling of copper reduction. *Water Research*, 39, 610–6.
- [40] Source Reduction Technologies in California. Printed Circuit Board Manufacture California Department of Toxic Substances Control Follow, 1-1999.
- [41] M. Burke (2007) The gadget scrap heap. *ChemWorld*, UK 4, 45–48.
- [42] Emery, A. (2002) A review of the UK metals recycling industry. *J.Waste Manage., Res.* 20, 457-467.
- [43] Widmer, R., Oswald-Krapf, H., Sinha-Khetriwal, D., Schnellmann, M., Böni, H. (2005) Global perspectives on e-scrap. *J. Environ., Impact Assess. Rev.*, 25, 436-458.
- [44] L.S. Roman, J. Puckett (2002) E-scrap exportation: challenges and considerations in *Proceedings of the IEEE International Symposium on Electronics and the Environment*, 79–84.
- [45] R. Widmer, H. Oswald-Krapf, D. Sinha-Khetriwal, M. Schnellmann, H. Böni (2005) Global perspectives on e-waste, *Environ. Impact. Assess. Rev.* 25, 436–458.

- [46] Zhang, Y., Liu, S., Xie, H., Zeng, X., Li, J. (2012) Current status on leaching precious metals from waste printed circuit boards, *Procedia Environ. Sci.*, 16, 560-568.
- [47] Workshop Materials on WEEE Management in Taiwan, Handout 10, (October 2012).
- [48] Telukdarie A, Brouckaert, Haung Y. (2006) A case study on artificial intelligence based cleaner Production evaluation system for surface treatment facilities. *Journal of Cleaner Production*, 14, 1622–34.
- [49] P. Williams, W. Hall(2007) Separation and recovery of materials from scrap printed circuit boards, *Resour. Conserv. Recycl.*, 51, 691–709.
- [50] Tang, X., Shen, C., Shi, D., Cheema, S.A., Khan, M.I., Zhang, C., Chen, Y. (2010) Heavy metal & persistent organic compound contamination in soil from Wenling: An emerging e-waste recycling city in Taizhou area, China. *J. Hazard. Mater.*, 173, 653-660.
- [51] J.W. Dini (1984) Fundamentals of chemical machining, *American Machinist*, Special Report 768, 113–128.
- [52] W.T. Harris (1974) *Chemical Milling*, Oxford University Press, UK.
- [53] R. Ueda (1989) Chemical machining with ferric chloride etchant. *Corros. Eng.* 38, 271–282.
- [54] D.M. Allen, O. Cakir (1993) Copper etching economics, *Photochem. Mach. Inst. J. (PCMI)*, (52), 4–7.
- [55] B. Fries (1999) *Source Reduction Technologies in California Printed Circuit Board Manufacture*. California Environmental Protection Agency.
- [56] Fitzpatrick-Brown AJ. (1985) Printed circuits: etching processes, *Electr Prod* 14, 28–30.
- [57] Mr. Robert E.S. Jr. (2002) Personal communication. Electronics business manager of MacDermid.
- [58] M.J. Thomas, “Etching”, *Technical Note (MacDermid (GB) Ltd.)* 28.
- [59] C.F. Coombs, Jr. (1995) *Printed Circuit Boards (Ed)*, McGraw-Hill.
- [60] R.E. Markle (1982) Etching to get ahead. *Ind. Finishing*, 58, 47–49.
- [61] Gurian M, Gilleo K, Murray J. (2000) Etched in our memories. *Printed Circuit Fabricat* 23, 116–26.
- [62] W.C. Bosshart (1985) “*Printed Circuit Boards- Design and Technology*”. Tata McGraw-Hill Publ.,
- [63] M. Georgiadou, R. Alkire (1993) Anisotropic chemical etching of copper coil: II. Experimental Studies on shape evaluation, *J. Elect. Soc.*, 140, 1348–1355.

- [64] Chemcut Corporation. Technical Information: Process Guidelines for Cupric Etching [web document]. Available: <http://www.chemcut.net/pdf/CupricChloride.pdf> (10.10. 2002).
- [65] R.E. Markle Industrial Finishing, 47-49, May (1982).
- [66] O. Çakir (1997) Proc. of the First Mechanical Engineering Congress, 464-468, 4-6 June Istanbul, Turkey.
- [67] Kenneth Mirski (1981) Proc.Tech. Prog. Nat. Electronic Pack. And Prod. Conf. 196-207, USA.
- [68] Chemcut Corporation. Technical Information: Process Guidelines for Alkaline Etching; bulletin 7, 1-16.
- [69] Queneau PB, Gruber RW (1997) The U.S. production of copper chemicals from secondary and by-product sources, JOM, 49, 34–37.
- [70] E.S. Robert Jr. (2002) personal communication. Electronics Business Manager of Mac Dermid, Current etchant market in Singapore,
- [71] HU Yao-hong, ZHAO Guo-peng (2009) Reuse treatment of spent copper-containing etching solution for printed circuit board. [J], Electroplating and Finishing 28 (10), 32-35 (in Chinese).
- [72] Printed Wiring Board On-Site Etchant Regeneration <http://www.p2pays.org/ref/10/09585> (2002)
- [73] Qian Yang, N.M. Kocherginsky (2006) Copper recovery and spent ammoniacal etchant regeneration based on hollow fiber supported liquid membrane technology: From bench- scale to pilot-scale tests. Journal of Membrane Science, 286, 301–309.
- [74] P.F. Atkins Jr., A. Scherger Dale (1997) A review of physical–chemical methods for nitrogen removal from wastewaters. Prog. Water Technol., 8, 713–720.
- [75] S.S. Banerjee, D.H. Chen (2007) J. Hazard. Mater., 147, 792.
- [76] A. Kortenkamp, M. Casadevall, S.P. Faux, A. Jenner, R.O.J. Shayer, N. Woodbrige, P. O'Brien, Arch (1996) Biochem. Biophys. 329 (2), 199.
- [77] K.W. Juang, H.Y. Lai, B.C. Chen (2011) Coupling bioaccumulation and phytotoxicity to predict copper removal by switchgrass grown hydroponically. Ecotoxicology, 20, 827–835.
- [78] J.S. Espana, E.L. Pamo, E.S. Pastor, J.R. Andres, J.A.M. Rubi (2006) The removal of dissolved metals by hydroxysulphate precipitates during oxidation and neutralization of acid mine waters. Aquat. Geochem, 12, 269–298.

- [79] D. Gjorgieva, T.K. Panovska, K. Baceva, T. Stafilov (2011) Assessment of heavy metal pollution in republic of Macedonia using a plant assay, *Arch. Environ. Contam. Toxicol.*, 60, 233–240.
- [80] S. Meiera, R. Azcónb, P. Cartesa, F. Boriea, P. Cornejoa (2011) Alleviation of Cu toxicity in *Oenothera picensis* by copper-adapted arbuscular mycorrhizal fungi and treated agro waste residue. *Appl. Soil Ecol.*, 48, 117–124.
- [81] B. Murphy, B. Hathaway, *Coord (2003) Chem. Rev.* 243, 237.
- [82] RAHMAN M S, ISLAM M R. (2009) Effects of pH on isotherms modeling for Cu (II) ions adsorption using maple wood sawdust. *Chemical Engineering Journal*, 149, 273-280.
- [83] S. Rengaraj, Y. Kim, C.K. Joo, J. Yi, J. (2004) *Colloid Interface Sci.*, 273, 14.
- [84] Ngah, W.S., Endud, C.S., Mayanar, R. (2002), “Removal of copper (II) ions from aqueous solution onto chitosan and cross-linked chitosan beads”. *React. Funct. Polym.*, 50 (5), 181-190
- [85] S.S. Djokic(1996). Cementation of copper on aluminum in alkaline solutions. *Journal of the electrochemical Society*, 143(4), 1300-1305.
- [86] Mecer process, <http://www.sigma-mercer.com>
- [87] G. Kyuchoukov, M.B. Bogacki, J. Szymanowski (1998) Copper extraction from ammoniacal solutions with LIX84 and LIX54. *Ind. Eng. Chem. Res.*, 37 (10), 4084–4089.
- [88] J. Hu, D. Shao, C. Chen, G. Sheng, J. Li, X. Wang, M. Nagatsu (2010) Plasma-induced grafting of cyclodextrin onto multiwall carbon nanotube/iron oxides for adsorbent application. *J. Phys. Chem.*, (B) 114, 6779–6785.
- [89] Moore MN (2006) Do nanoparticles present ecotoxicological risks for the health of the aquatic environment? *Environ Int.*, 32, 967-976.
- [90] Boyer, C., Whittaker, M.R., Bulmus, V., Liu, J., Davis, T.P. (2010) The design and utility of polymer-stabilized iron oxide nanoparticles for nanomedicine applications. *NPG Asia Mater.*, 2, 23–30.
- [91] B.R. White, B.T. Stackhouse, J.A. Holcombe (2009) Magnetic gamma-Fe₂O₃ nanoparticles coated with poly-l-cysteine for chelation of As(III), Cu(II), Cd(II), Ni(II), Pb(II) and Zn(II), *J. Hazard. Mater.*, 161, 848–853.
- [92] L.Carlos, F.S. García Einschlag, M.C. González, D.O. Mártire (2013) Applications of magnetite nanoparticles for heavy metal removal from wastewater: In *Waste Water – Treatment Technologies and Recent Analytical Developments*. InTech, Rijeka, 63–78.

- [93] Cornell R.M and Schwertmann (2003) The iron oxide: Structure, Properties, Reactions, Occurrences and Uses, Wiley-VCH gmbh & Co. Kga, 2nd edition, 694.
- [94] Teja AS, Koh PY (2009) Synthesis, properties, and applications of magnetic iron oxide Nanoparticles, Prog Cryst Growth, Ch. 55, 22-45.
- [95] Pankhurst QA, Thanh NTK, Jones SK, Dobson J. (2009) Progress in applications of magnetic nanoparticles in biomedicine. J Phys D Appl Phys, 42
- [96] Qiao RR, Yang CH, Gao MY. (2009) Superparamagnetic iron oxide nanoparticles: from preparations to *in vivo* MRI applications. J Mater Chem., 19, 6274-6293.
- [97] Murillo TP, Sandquist C, Jacobs PM, Nesbit G, Manninger S, Neuwelt EA (2005) Imaging brain tumors with ferumoxtran-10: a nanoparticle magnetic resonance contrast agent. Therapy 2, 871-882
- [98] Geppert M. (2012) Synthesis and characterization of iron oxide nanoparticles and investigation of their biocompatibility on astrocyte cultures. PhD thesis, University of Bremen, Bremen, Germany
- [99] Yu J, Huang DY, Yousaf MZ, Hou YL, Gao S. (2013) Magnetic nanoparticle-based cancer therapy. Chinese Phys B, 22
- [100] Karn B, Kuiken T, Otto M. (2009) Nanotechnology and *in situ* remediation: a review of the benefits and potential risks. Environ Health Perspect, 117, 1813-31.
- [101] Crane RA, Scott TB (2012) Nanoscale zero-valent iron: future prospects for an emerging water treatment technology. J. Hazard Mater., 211-212, 112-25.
- [102] Tang SCN, Lo IMC (2013) Magnetic nanoparticles: Essential factors for sustainable environmental applications. Water Research, 47, 2613-2632
- [103] Wang C-B, Zhang W-x (1997) Synthesizing nanoscale iron particles for rapid and complete dechlorination of TCE and PCBs. Environmental Science & Technology, 31, 154-2156
- [104] Carpenter E. E. (2001) Iron nanoparticles as potential magnetic carriers. Journal of Magnetism and Magnetic Materials, 225, 17–20.
- [105] John Wiley & Sons (2003) Inc., Hoboken, New Jersey.
- [106] Y.F. Shen, J. Tang, Z.H. Nie, Y.D. Wang, Y. Ren, L. Zuo (2009) Preparation and application of magnetic Fe₃O₄ nanoparticles for wastewater purification. Sep. Sci. Technology, 68, 312- 319.

- [107] J.F. Liu, Z.S. Zhao, G.B. Jiang (2008) Coating Fe₃O₄ magnetic nanoparticles with humic acid for high efficient removal of heavy metals in water. *Environ. Sci. Technol.*, 42, 6949-6954.
- [108] Y.T. Zhou, H.L. Nie, C. Branford-White, Z.Y. He, L.M. Zhu (2009) Removal of Cu²⁺ from aqueous solution by chitosan-coated magnetic nanoparticles modified with alpha-ketoglutaric acid. *J. Colloid. Interface Sci.*, 330, 29–37.
- [109] <http://www.hindawi.com/journals/jnt/2014/398569>
- [110] Mark R. Wiesner, Jean-Yves Bottero (2007), *Environmental Nanotechnology: Application and Impacts of Nanomaterials*, Mark R. Wiesner, P.E., Jean-Yves Bottero Editors, McGraw-Hill Companies, U.S.A.
- [111] Reynolds, T. D., and Richards, P. A. (1996) *Unit Operations and Processes in Environmental Engineering*, 2nd ed., PWS Publishing Company, Boston, MA.
- [112] Stumm, W., James J. Morgan, J.,J. (1996) *Aquatic Chemistry: Chemical Equilibria and Rates in Natural Waters*, John, Wiley and sons Inc., New York ,USA.
- [113] Lin, S., S. (1997) Interaction of H₂O₂ with iron oxide for oxidation of organic compounds in water. Ph.D. thesis, Drexel Univ., Philadelphia, USA.
- [114] <http://www.mmrc.caltech.edu/FTIR/FTIRintro.pdf>
- [115] Shetty AR (2006) Metal anion removal from wastewater using chitosan in a polymer enhanced diafiltration system, A Thesis submitted to the Faculty of Worcester Polytechnic Institute, Degree of Master of Science in Biotechnology.
- [116] C. Wilaiwan, S. Yongsoon, D. Joseph, D.S. William, H.L. Nikki, D.R. Ryan, E.F. Glen, S. Thanapon, Y. Wassana (2010) Selective removal of copper (II) from natural waters by Nanoporous sorbents functionalized with chelating diamine. *Environ. Sci. Technol.*, 44, 6390–6395.
- [117] J.H. Wang, S.R. Zheng, Y. Shao, J.L. Liu, Z.Y. Xu, D.Q. Zhu (2010) Aminofunctionalized Fe₃O₄@SiO₂core–shell magnetic nanomaterial as a novel adsorbent for aqueous heavy metals removal. *J. Colloid Interface Sci.*, 349, 293–299.
- [118] J.F. Liu, Z.S. Zhao, G.B. Jiang (2008) Coating Fe₃O₄ magnetic nanoparticles with humic acid for high efficient removal of heavy metals in water. *Environ. Sci. Technol.*, 42, 6949–6954.
- [119] S. Singh, K.C. Barick, D. Bahadur (2011) Surface engineered magnetic nanoparticles for removal of toxic metal ions and bacterial pathogens. *J. Hazard. Mater.*, 192, 1539–1547.
- [120] T. Fan, Y. Liu, B. Feng, G. Zeng, C. Yang, M. Zhou, H. Zhou, Z. Tan, X. Wang (2008), Biosorption of cadmium (II), zinc (II) and lead (II) by *Penicillium simplicissimum*: isotherms, kinetics and thermodynamics. *J. Hazard. Mater.*, 160, 655– 661.

- [121] Z. Rawajfih, N. Nsour (2008) Thermodynamic analysis of sorption isotherms of chromium (VI) anionic species on reed biomass. *J. Chem. Thermodynamics*, 40, 846–851.
- [122] S. Erenturk, E. Malkoc (2007) Removal of lead (II) by adsorption onto *Viscum album*: Effect of temperature and equilibrium isotherm analyses. *Appl. Surf. Sci.*, 253, 4727–4733.
- [123] Hao, Y., Man, C. Hu, Z. (2010) Effective removal of Cu (II) ions from aqueous solution by amino-functionalized magnetic nanoparticles. *Journal of Hazardous Materials*, 184, 392-399.
- [124] Zhan, J.Y., Tian, G.F., Jiang, L.Z., Wu, Z.P., Wu, X.P., Yang, R.G. (2008) Superparamagnetic polyimide/ γ -Fe₂O₃ nanocomposite films: preparation characterization, *Thin Solid Films* 516
- [125] Hu, J., Chen, G. H., Lo, I.M.C. (2006) Selective removal of heavy metals from industrial waste water using maghemite nanoparticle: performance and mechanisms. *Journal of Environ. Eng.*, 132, 709–715.
- [126] Peng, Q., Liu, Y., Zeng, G., Xu, W., Yang, C., Zhang, J. (2010) Biosorption of copper (II) by immobilizing *Saccharomyces cerevisiae* on the surface of chitosan-coated magnetic nanoparticles from aqueous solution. *Journal of Hazardous Materials*, 177, 676-682.
- [127] Yan, H., Yang, L., Yang, Z., Yang, H., Li, A., Cheng, R. (2012) Preparation of Chitosan/poly (acrylic acid) magnetic composite microspheres and applications in the removal of copper (II) ions from aqueous solutions. *Journal of Hazardous Materials*, 229-230, 371-380.
- [128] Shashwat S. Banerjee, Dong-Hwang Chen (2007) Fast removal of copper ions by gum Arabic modified magnetic nano-adsorbent. *Journal of Hazardous Materials*, 147, 792–799.
- [129] Reza Bazargan-Lari, Hamid Reza Zafarani, Mohammad Ebrahim Mahrololom, Afshi Nemati (2014) Removal of Cu(II) ions from aqueous solutions by low-cost natural hydroxyapatite/chitosan composite: Equilibrium, kinetics and thermodynamic studies. *Journal of the Taiwan Institute of Chemical Engineers*, 1642-1648.
- [130] J.F. Liu, Z.S. Zhao, G.B. Jiang (2008) Coating Fe₃O₄ magnetic nanoparticles with humic acid for high efficient removal of heavy metals in water, *Environ. Sci. Technol.*, 42, 6949–6954.
- [131] Natálie C. Feitoza, Thamires D. Gonçalves, Jéssica J. Mesquita, Jucely S. Menegucci, Mac-Kedson M.S. Santos, Juliano A. Chaker, Ricardo B. Cunha, Anderson M.M. Medeiros, Joel C. Rubim, Marcelo H. Sousa (2014) Fabrication of glycine-functionalized maghemite nanoparticles for magnetic removal of copper from wastewater. *Journal of Hazar. Mater.*, 264, 153– 160.

- [132] S. Deng, R. Bai, J.P. Chen (2003) Aminated polyacrylonitrile fibers for lead and copper removal. *Langmuir*, 19, 5058–5064.
- [133] GIRI J., THAKURTA S.G., BELLARE J., NIGAM A.K., BAHADUR D. (2005) J., *Magn. Mater.*, 293, 62.
- [134] AHN Y., CHOI E.J., KIM E.H. (2003) *Rev. Adv Mater. Sci.*, 5, 477.
- [135] Liu, S., Aquino, A. J. A., Korzeniewski, C. (2013) Water-ionomer interfacial interactions investigated by infrared spectroscopy and computational methods. *Langmuir*, 29, 13890- 13897.
- [136] M. Monier, D.M. Ayad, Y. Wei, A.A. Sarhan (2010) Preparation and characterization of magnetic chelating resin based on chitosan for adsorption of Cu(II), Co(II), & Ni(II) ions. *React. Funct. Polym.*, 70, 257–266.
- [137] G.Y. Li, K.L. Huang (2008) Preparation and characterization of *Saccharomyces cerevisiae* alcoholdehydrogenase immobilized on magnetic nanoparticles. *Int. J. Biol. Macromol.*, 42, 405–412.
- [138] P. Kolhe and R. M. Kannan (2003) *Biomacromolecules*, 4, 173.
- [139] S. Hong and I. Rhee (2007) *J. Korean Phys. Soc.*, 51, 1453.
- [140] K. Nakamoto (1997) *Infrared and Raman spectra of inorganic and coordination compounds*, John Wiley & Son, New York,
- [141] REN Y., LIMURA K., KATO T. (2001) *Langmuir*, 17, 2688.
- [142] Turaga U., Singh V., Behrens R., Korzeniewski C., Jinka S., Smith E., Kendall R. J., Ramkumar S. (2014) Breathability of standalone poly (vinyl alcohol) nanofiber webs. *Ind. Eng. Chem. Res.*, 53, 6951-6958.
- [143] Li P, Yu B, Wei X (2004) Synthesis and characterization of a high oil-absorbing magnetic composite material. *Journal of applied polymer science*, 93 (2), 894–900.
- [144] Mahesh D. Bedre, Raghunandan D, Basavaraja S, Balaji D.S, Arunkumar Lagashetty and Venkataraman A. (2010) “Preparation and characterization of magnetic Fe₂O₃” *J. Metal. & Mat. Sci.*, V.52, 209-214.
- [145] T. Agarwal, K. A. Gupta, S. Alam, M. G. H. Zaidi (2012) Fabrication and Characterization of Iron Oxide Filled Polyvinyl Pyrrolidone Nanocomposites. *International Journal of Composite Materials*, 2(3), 17-21.
- [146] Andra PREDESCU, Avram NICOLAE (2012) ADSORPTION OF ZN, CU AND CD FROM WASTE WATERS BY MEANS OF MAGHEMITE NANOPARTICLES. *U.P.B. Sci.*

Bull., Series B, Vol. 74, Iss. 1.

[147] A.Z.M. Badruddoza, A.S.H. Tay, P.Y. Tan, K. Hidajat, M.S. Uddin (2011) Carboxymethyl- β -cyclodextrin conjugated magnetic nanoparticles as nano-adsorbents for removal of copper ions Synthesis and adsorption studies. *Journal of Hazardous Materials*, 185, 1177-1186.

[148] A.Z.M. Badruddoza, K. Hidajat, M.S. Uddin (2010) Synthesis and characterization of beta-cyclo-dextrin-conjugated magnetic nanoparticles and their uses as solid phase artificial chaperones in refolding of carbonic anhydrase bovine. *J. Colloid Interface Sci.*, 346, 337–346.

CURRICULUM VITAE

Name Surname : Oumer Ali Yassin
Date of Birth : 17.06.1983
Place of Birth : Dessie, Ethiopia
Foreign Language : Arabic, English, Turkish
E-mail : oumersemera@yahoo.com

Education:

Degree	Department	University	Graduation Year
First Degree	Biology	Dilla, Ethiopia	2006
Master Degree	Environmental Engineering	Marmara, Turkey	2016

Work Experience:

Year	Foundation & Country	Duty/Responsibility
2006-2008	Kebena Secondary School, Ethiopia	Biology Teacher
2009-2010	Samara University, Ethiopia	Graduate Assistance
2016	English Time, Istanbul/Turkey	Turkish Language (For Syrian refugees)
2016	Mevlana Celebi İlim ve Hizmet vakıf, Istanbul/Turkey	English Teacher

Conference Proceeding

Oumer Ali Yassin, Gül Gülenay Hacıosmanoğlu, Seval Genç, Ebru Toksoy Öner, Zehra Semra Can (2016) Copper Removal from Ammoniacal Spent Etchant Using Magnetic Nanoparticles. 3rd EurAsia Waste Management Symposium, 2-4 may 2016, Istanbul, Turkey.